Robust decentralized optimization of Multi-Microgrids integrated with Power-to-X technologies

Mansour-Saatloo, Amin ; Pezhmani, Yasin ; Mirzaei, Mohammad Amin ; Mohammadiivatloo, Behnam; Zare, Kazem; Marzband, Mousa; Anvari-Moghaddam, Amjad

Published in:
Applied Energy

DOI (link to publication from Publisher):
10.1016/j.apenergy.2021.117635

Publication date:
2021

Document Version
Accepted author manuscript, peer reviewed version

Robust Decentralized Optimization of Multi-Microgrids integrated with Power-to-X Technologies

Amin Mansour-Saatloo[1], Yasin Pezhmani[1], Mohammad Amin Mirzaei[1], Behnam Mohammadi-Ivatloo[1, 3], Kazem Zare[1*], Mousa Marzband[2,3], Amjad Anvari-Moghaddam[4, 1]

[1]Faculty of Electrical and Computer Engineering, University of Tabriz, Tabriz, Iran

[2]Northumbria University, Electrical Power and Control Systems Research Group, Ellison Place NE1 8ST Newcastle upon Tyne, United Kingdom

[3]Center of Research Excellence in Renewable Energy and Power Systems, King Abdulaziz University, Jeddah 21589 Saudi Arabia

[4]Department of Energy Technology, Aalborg University, 9220 Aalborg, Denmark

*Email: kazem.zare@tabrizu.ac.ir

***Abstract*—** Nowadays, the enormous rising demand for hydrogen fuel cell vehicles (HFCVs) and electric vehicles (EVs) in the transportation sector has a significant contribution in growing of multi-energy microgrids (MEMGs) accompanied by hydrogen refueling stations (HRSs), EV parking lots (EVPLs) and power-to-hydrogen ($P2H_2$) technologies. The competency to enhance the efficiency and the reliability in MEMG systems leads to form a networked structure called multi-microgrids (MMG). In this paper, a robust decentralized energy management framework is proposed for the optimal day-ahead scheduling of a set of interconnected hydrogen, heat, and power-based microgrids (MGs) in the presence of HRSs and EVPLs. The proposed MMG is a collaborative structure of hydrogen provider company (HPC) and electricity markets with novel technologies such as power-to-heat (P2H), power-to-hydrogen ($P2H_2$), combined heat and power (CHP) units, multiple energy storages and demand response to improve the system flexibility in meeting multi-energy demands. The necessity of data privacy preservation methods for MGs has emerged when the interconnected MGs are operated as an MMG to satisfy different energy demands with minimum cost. Therefore, an iterative-based algorithm called the alternating direction

method of multipliers (ADMM) is utilized to decompose the structure of the scheduling problem to minimize the total daily cost of the MMG system while protecting the data privacy of MEMGs. In the proposed structure, the robust optimization model is able to manage the uncertainty by considering the worst-case scenario for electricity price in different conservativeness levels as MEMGs are sensitive to electricity price fluctuations. Finally, the simulation results represent the effectiveness of the proposed decentralized model under the worst case of electricity market price to meet the demand for electricity, heat, and hydrogen.

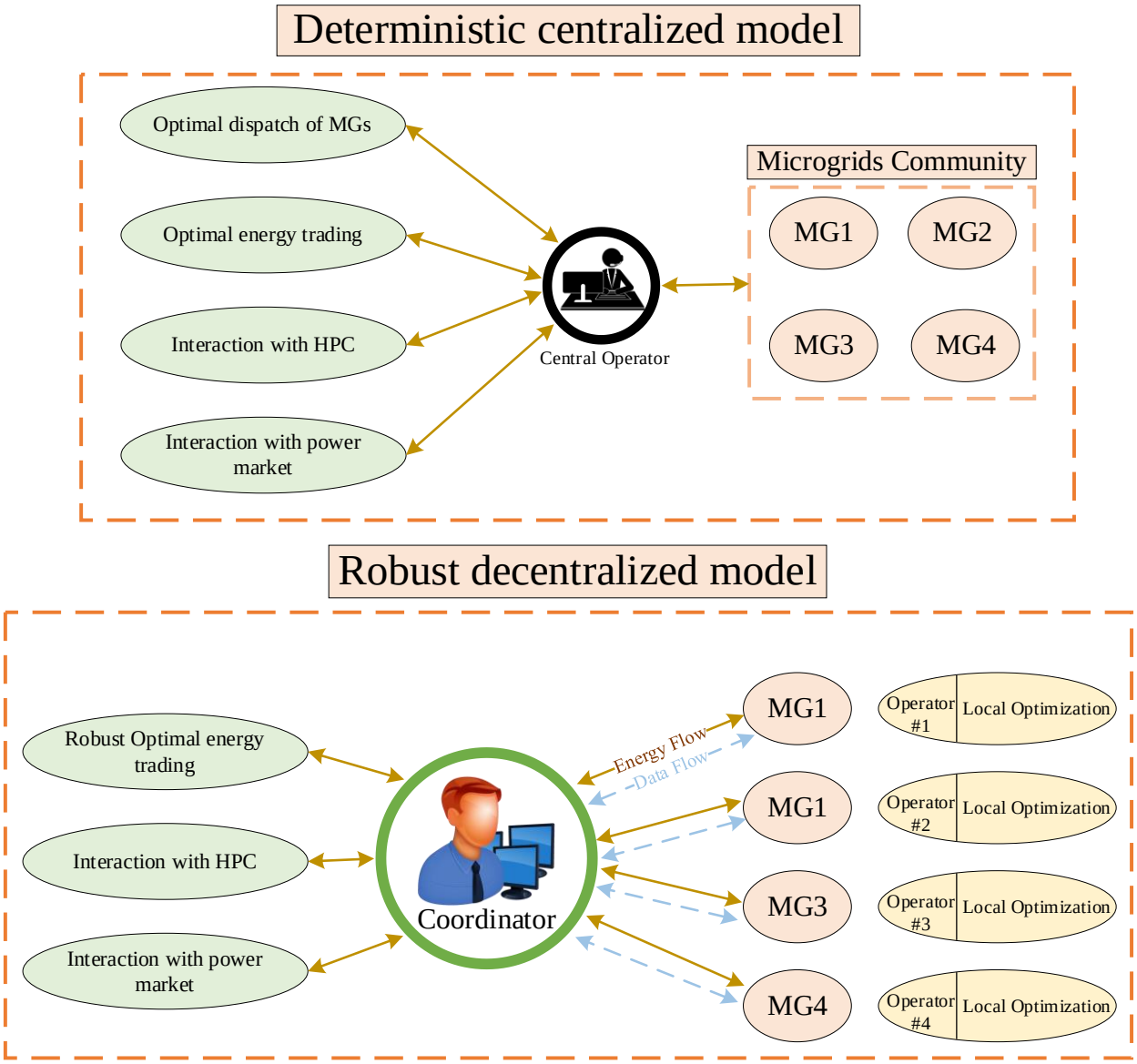

Graphical abstract

***Index Terms*—Multi-energy system, multi-microgrid hydrogen refueling station, electric vehicle, power to hydrogen technology, robust optimization.**

Acronyms

HRS	Hydrogen refueling station
EVPL	Electrical vehicle parking lot
HFCV	Hydrogen fuel cell vehicle
EV	Electric vehicle

DR	Demand response
RO	Robust optimization
ADMM	Alternating direction method of multipliers
$P2H_2$	Power to hydrogen
P2H	Power to heat
H2P	Hydrogen to power
MEMG	Multi-energy microgrid
MG	Microgrid
MMG	Multi-microgrids
CHP	Combined heat and power
FOR	Feasible operation region
PV	Photovoltaic
WT	Wind turbine
ESS	Electrical storage system
TSS	Thermal storage system
HSS	Hydrogen storage system
DER	Distributed energy resources
RES	Renewable energy sources
HPC	Hydrogen provider company

Index

t	Time Period
m	Multi-energy microgrid
J	Electrical vehicle type
K	Electrical vehicle cluster

Constants and parameters:

N_m^{wt}	Number of WTs
N_m^{pv}	Number of PV panels
N_m^{EV}	Number of EVs

Nm	Number of MEMGs
M	A sufficient large number
λ_t^{el}	Electrical energy price ($/MWh)
λ_t^{hd}	Heat price ($/MWth)
$P_{t,m}^{load}, T_{t,m}^{load}$	Electrical/thermal demand of MEMG *m* at hour *t* before DR programs (MW/MWth)
$H_{t,m}^{HRS}$	Hydrogen demand of HRS at MEMG *m* at hour *t* (kg)
$H_{t,m}^{load}$	Hydrogen demand of MEMG *m* at hour *t* (kg)
$a_m, b_m, c_m, d_m, e_m, f_m$	Cost coefficients of CHP at MEMG *m*
C_m^{su}, C_m^{sd}	Start-up/shut-down cost of CHP at MEMG *m* ($)
SUC_m / SDC_m	Start-up/Shut-down constant costs ($)
$\alpha_m, \beta_m, \gamma_m$	Cost function coefficients of gas boiler at MEMG *m*
$T_m^{bo,\max}$	Maximum heat produced by gas boiler at MEMG *m* (MWth)
$\eta_m^{P2H}, \eta_m^{P2H_2}, \eta_m^{H2P}$	Efficiency of P2H/P2H$_2$/H2P technology
$T_m^{P2H,\max}$	Maximum heat produced by P2H technology at MEMG *m* (MWth)
$\eta_m^{ch,ES}, \eta_m^{disch,ES}$	Charging/discharging efficiency for ESS of MEMG *m*
$\underline{P}_m^{ch,ES}, \overline{P}_m^{ch,ES}$	Lower/upper bound for ESS charging power of MEMG *m* (MW)
$\underline{P}_m^{disch,ES}, \overline{P}_m^{disch,ES}$	Lower/upper bound for ESS discharging power of MEMG *m* (MW)
$SoC_m^{\min,ES}, SoC_m^{\max,ES}$	Lower/upper bound for ESS stored energy of MEMG *m* (MW)
$\eta_m^{ch,TS}, \eta_m^{disch,TS}$	Charging/discharging efficiency for TSS of MEMG *m*
$\underline{T}_m^{ch,TS}, \overline{T}_m^{ch,TS}$	Lower/upper bound for TSS charging power of MEMG *m* (MWth)
$\underline{T}_m^{disch,TS}, \overline{T}_m^{disch,TS}$	Lower/upper bound for TSS discharging power of MEMG *m* (MWth)
$SoC_m^{\min,TS}, SoC_m^{\max,TS}$	Lower/upper bound for TSS stored energy of MEMG *m* (MWth)
$P_m^{P2H_2,\max}$	Maximum power consumed by P2H$_2$ technology at MEMG *m (*MW*)*
$\eta_m^{ch,HS}, \eta_m^{disch,HS}$	Charging/discharging efficiency for HSS of MEMG *m*
$\underline{H}_m^{ch,HS}, \overline{H}_m^{ch,HS}$	Lower/upper bound for HSS charging power of MEMG *m* (kg)

$\underline{H}_m^{disch,HS}, \bar{H}_m^{disch,HS}$	Lower/upper bound for HSS discharging power of MEMG *m* (kg)
$SoC_m^{\min,HS}, SoC_m^{\max,HS}$	Lower/upper bound for HSS stored energy of MEMG *m* (kg)
$\eta_{m,j}^{ch,EV}, \eta_{m,j}^{disch,EV}$	Charging/discharging efficiency for EV of MEMG *m*
$SoC_{m,j}^{EV,\min}, SoC_{m,j}^{EV,\max}$	Lower/upper bound for EV stored energy of MEMG *m* (MW)
$\underline{P}_{m,j}^{ch,EV}, \bar{P}_{m,j}^{ch,EV}$	Lower/upper bound for EV charging power of MEMG *m* (MW)
$\underline{P}_{m,j}^{disch,EV}, \bar{P}_{m,j}^{disch,EV}$	Lower/upper bound for EV discharging power of MEMG *m* (MW)
R_k	Probability of each cluster
Q_j	Coefficient for determining the number of EV types
$\underline{H}_m^{H2P}, \bar{H}_m^{H2P}$	Minimum/maximum hydrogen consumed by H2P technology at MEMG *m* (kg)
$\underline{P}_m^{H2P}, \bar{P}_m^{H2P}$	Minimum/maximum power produced by H2P technology at MEMG *m* (MW)
LHV_m	Lower heating value of hydrogen
P_{rated}^{wt}	Rated power of WTs (MW)
$v_{in}^c, v_{out}^c, v_{rated}$	Cut-in, Cut-out, and nominal wind speed (m/s)
v_t	Wind speed (m/s)
AT_t	Ambient temperature at hour t (°C)
T_{C_t}	PV panel temperature at hour t (°C)
V_{oc}	Open circuit voltage of PV panels (V)
I_{sc}	Short circuit current of PV panels (A)
K_i, K_v	Current/voltage temperature coefficient of PV panels (A/°C)/(V/°C)
I_{MPP}, V_{MPP}	Current/voltage at maximum power point of PV panels (A)/(V)
FF	Fill factor of PV panel
N_{OT}	Rated operating temperature of PV panels (°C)
$sor_{t,m}$	Solar radiation at hour t (kW/m^2)
D_m^{inc}, D_m^{curt}	Coefficient of load shift up/down in DR programs

Binary Variables:

$X_{t,a}, X_{t,b}$	The operation state for the CHP of MEMG *m* in first/second convex sub-region of the FOR
$V_{t,m}^{chp}$	Commitment status for CHP of MEMG *m*
$SU_{t,m}^{chp}, SD_{t,m}^{chp}$	Start-up/shut-down status for CHP of MEMG *m*
$I_{t,m}^{ch,ES}, I_{t,m}^{disch,ES}$	Charging/discharging status for ESS of MEMG *m*
$I_{t,m}^{ch,TS}, I_{t,m}^{disch,TS}$	Charging/discharging status for TSS of MEMG *m*
$I_{t,m}^{ch,HS}, I_{t,m}^{disch,HS}$	Charging/discharging status for HSS of MEMG *m*
$I_{t,m,j,k}^{ch,EV}, I_{t,m,j,k}^{disch,EV}$	Charging/discharging status for EV of MEMG *m*

Decision variables:

$P_{t,m}^{load}, T_{t,m}^{load}$	Electrical/thermal demand of MEMG *m* at hour *t* after DR programs (MW/MWth)
$P_{t,m}^{inc}, P_{t,m}^{curt}$	The amount of increased/curtailed electrical load in electrical DR program (MW)
$T_{t,m}^{inc}, T_{t,m}^{curt}$	The amount of increased/curtailed thermal load in thermal DR program (MWth)
P_{t}^{EM-Co} / H_{t}^{EM-Co}	Exchanged power/hydrogen between multi-energy market and the coordinator (MW)/(kg)
$C_{t,m}^{chp}$ / $C_{t,m}^{bo}$	Cost function of CHP / gas boiler ($/h)
$C_{t,m}^{opr}$	Operation cost of CHP ($/h)
$P_{t,m}^{chp}$ / $T_{t,m}^{chp}$	Power/heat generation of CHP *(*MW)/(MWth)
T_{m}^{bo}, T_{m}^{P2H}	Thermal energy produced by gas boiler / P2H technology (MWth)
$P_{t,m}^{ch,ES}, P_{t,m}^{disch,ES}$	Charging/discharging power for ESS of MEMG *m* (MW)
$SoC_{t,m}^{ES}, SoC_{t,m}^{TS}, SoC_{t,m}^{HS}$	Stored energy for ESS/TSS/HSS of MEMG *m* (MW)/(MWth)/(kg)
$T_{t,m}^{ch,TS}, T_{t,m}^{disch,TS}$	Charging/discharging power for TSS of MEMG *m* (MWth)
$H_{t,m}^{ch,HS}, H_{t,m}^{disch,HS}$	Charging/discharging power for HSS of MEMG *m* (kg)
$P_{t,m}^{P2H}, P_{t,m}^{P2H_2}$	Consumed power by P2H/P2H_2 facility of MEMG *m* (MW)
$H_{t,m}^{P2H_2}$	Produced hydrogen by P2H_2 technology of MEMG *m* (kg)

$P_{t,m,j,k}^{ch,EV}, P_{t,m,j,k}^{disch,EV}$	Charging/discharging power for EV of MEMG *m* (MW)
$SoC_{t,m,j,k}^{EV}$	Stored energy for EV of MEMG *m* (MW)
$H_{t,m}^{H2P}$	Consumed hydrogen by H2P facility of MEMG *m* (kg)
$P_{t,m}^{H2P}$	Produced power by H2P technology of MEMG *m* (MW)
$P_{t,m}^{WT}, P_{t,m}^{PV}$	Produced power by WT/PV (MW)
$P_{t,m}^{MEMG-Co}, P_{t,m}^{Co-MEMG}$	Exchanged power between each MEMG and the coordinator (MW)
$H_{t,m}^{MEMG-Co}, H_{t,m}^{Co-MEMG}$	Exchanged hydrogen between each MEMG and the coordinator (kg)

1. Introduction

1.1. Overview

The dramatic growth of the urban population during the past couple of decades has created new environmental challenges for humankind. According to a report published by the United States environmental protection agency, the electricity production and transportation sectors are responsible for 55% of total emissions just in 2018 [1]. Therefore, in order to achieve decarbonatization, it is essential to use green energies across all sectors. In recent years, the acceleration of environmentally friendly technologies such as electric vehicles (EVs) and hydrogen fuel cell vehicles (HFCVs) is now being considered to replace fossil fuel vehicles. Therefore, several vehicle manufacturing giants such as Toyota Motor Corporation, Fiat Chrysler Automobiles, and Nissan Motor Corporation have been more focused on prioritizing mass production of HFCVs [2]. Renewable energy sources (RES) have a pivotal role in the transition from fossil fuel vehicles to EVs and HFCVs due to the fact that the energy for EVs and HFCVs could be provided directly or indirectly from wind turbines (WTs) or photovoltaic (PV) panels [3].

Nowadays, development in Power-to-hydrogen ($P2H_2$) technology have made the hydrogen utilization process more straightforward. Hydrogen is considered as an important energy carrier that can be easily generated through water electrolysis. During electrolysis, electricity is consumed, and as a result, oxygen

and hydrogen are produced. If the electricity consumed during the hydrogen production process is provided by RES, hydrogen can be considered as a clean and flexible energy carrier [4]. Project Pilbara region, Australia and project Victoria, British Columbia are some of the hydrogen projects that have been done to utilize hydrogen. Europe's largest green hydrogen project in Groningen, the Netherlands, has been scheduled to be used at the end of 2020 [5].

Rapidly increasing of distributed energy resources (DER) such as combined heat and power (CHP) in overall electricity production had improved the flexibility of the energy systems. Due to the ability to produce power and heat simultaneously, CHP can enhance the efficiency of power systems. Moreover, using CHP for heat and power production could decrease pollutant gas emission by 13% to 18% [6]. With the rapid penetration of DER in power systems throughout the world, the idea of microgrid (MG) has become an interesting research issue. MG can be defined as an electrical distribution network that consists of energy storage systems, flexible and inflexible loads, and distributed generations. MGs can be operated in two distinct modes, i.e., isolated mode and interconnected mode. However, applying the interconnected mode of MGs could improve system reliability and performance [7, 8]. Due to the advantages such as improved energy utilization efficiency, the propensity to integrate different energy carriers such as hydrogen, heat, and electricity into MGs' traditional structure has increased rapidly over the past few years [9]. Hence the multi-microgrids (MMGs) systems, which are a combination of several energy resources and energy consumers, were introduced. Multi microgrids can improve the satisfaction factor of both the MGs operators and customer by reducing operational costs and providing reliable energy [8, 10].

1.2. Literature review

In this section, several related studies on the energy management of MMGs are discussed in depth. In [11], optimal power management of a set of multi-carrier networked MGs in an uncertain environment has been considered where a novel time-based demand-side management is used to change the load curve and to prevent excess energy consumption during peak hours. In [12], a bi-level energy management system has been proposed for an isolated structure of renewable-based MMGs where scenario generation

is used to control the uncertainties of loads and renewable generations. The authors in [13] have used a chance-constrained model for stochastic optimal day-ahead scheduling of an MMG considering the global policy for emissions reduction. In [14] for an active distribution network, a privacy-preserving energy management approach has been presented. Moreover, in [14] a generalized Benders decomposition is used to solve the energy management problem in a decentralized model. The authors in [15] have investigated the effect of survivability-oriented demand response (DR) program on energy management of a network of MGs where the uncertainties of load and renewable resources are controlled by using a robust optimization (RO) method. A decentralized energy management model has been proposed in [16], where the alternating direction method of multipliers is applied to coordinate the power exchange between networked MGs and distribution systems. In [17], a stochastic multi-objective model for optimal energy management of networked MMGs has been presented in which DR programs are implemented to mitigate the total daily costs of the MMG operator. In [18], two kinds of decentralized energy management framework have been described for coordinated operation between MGs and distribution network. Moreover, in [18] column and constraint generation algorithm has been used to solve the economic dispatch problem in a decentralized way. A novel decentralized-distributed adaptive robust optimization method for AC/DC hybrid MMG scheduling has been proposed in [19], where a novel altering optimization procedure-looped Column-and-constraint generation algorithm is developed to determine the robust optimal plans of multiple stakeholders. In [20], a distributional robust predictive control approach for real-time distributed optimal power flow of a MMG has been proposed in which the operational independence of MGs is preserved by devising a decomposition scheme that is based on the alternating direction method of the multipliers (ADMM) algorithm and modified column-and-constraint generation method.

Many research papers have focused on multi-energy microgrids (MEMGs) in recent years due to the potential MEMGs possess. A risk-averse hybrid approach has been used in [5] for optimal scheduling of a MEMG, where the $P2H_2$ technology and the multi-energy storage systems boost the system efficiency. Robustly coordinated operation of a MEMG has been studied in [21], where flexible thermal and

electrical loads, combined cooling, heat, and power plants and thermal storage are optimally coordinated by using a two-stage coordinated operation model. In [22], a system-wide optimal coordinated dispatch model for a MEMG in islanded and grid-connected modes has been proposed where the dispatch interactions between heat/cooling and power are improved significantly by utilizing electrical chillers and electrical boilers. In [23], the coordinated scheduling and optimal operation strategy of a MEMG has been studied for flexibility enhancement considering the implementation of power to gas technology and cogeneration technology. In [24], a stochastic-robust coordinated optimization model has been proposed for a MEMG, where the uncertainty of renewable generations and power market prices are taken into account. The authors in [25] have proposed a hybrid optimization technique for economic and environmental assessment of a renewable-based MEMG integrated with flexible technologies. A two-stage coordinated scheduling model to deal with the optimization problem of a MEMG has been proposed in [26], where a chaotic cell membrane-particle swarm optimization algorithm is employed to solve the proposed model.

The studies on the utilization of EVs and HFCVs can be found in the literature. A scheduling model of an MG with hydrogen refueling stations (HRSs) has been investigated in [27], where the uncertainties of electricity price, hydrogen and electrical load, and renewable generation are taken into account. The authors in [28] have introduced a hybrid fuel station powered by PV panels to supply both HFCVs and EVs, adopting a stochastic method to handle the uncertainties. In [29], a novel supervisory-based model has been proposed to achieve optimal scheduling of distributed HRSs, where their capacity is optimally shared between the transportation sector and the operating reserve in electricity markets. A novel model for optimal scheduling of electrolyzer-based HRSs has been proposed in [30], where a capacity-based DR program is implemented to intensify the system profit. In [31], a MG with fuel cell electric vehicles, wind turbines, and photovoltaic systems has been presented in which the fuel cell electric vehicles are utilized to provide vehicle-to-grid power during low renewable generation periods. The end-users' potential to utilize fuel cell electric vehicles in vehicle-to-grid operation for acting as a local power supply has been

evaluated in [32]. In [33] a new hierarchical stochastic control model has been shown to coordinate plug-in electric vehicles and wind turbine in an MG in which the aggregated charging power to each plug-in electric vehicle is optimally allotted by using the presented model. The authors in [34] have used a bi-level programming model to incorporate DR of EVs for achieving optimal scheduling of renewable-based isolated MGs.

1.3. Research gaps and contributions

To the best of the authors' knowledge, there are no studies that focus on the optimal scheduling of combined heat, power and hydrogen-based MMGs to meet multi-energy demands while preserving MGs' privacy. According to the enlisted literature, the following research gaps exist:

- Some papers such as [22, 33] have developed scheduling models for only a single microgrid without considering hydrogen, while a community of microgrids, i.e., multi microgrids, integrated with hydrogen facilities has potential to improve the flexibility, security and reliability of both microgrids and the power grid.
- There were a plenty of works, e.g., [11, 13, 15], which have presented scheduling models for multi microgrids, yet it has been considered that they are operated under a central operator; however, in real world, each microgrid might has its own operator and an individual operator do not willing to share data with any third party. Therefore, these models can not be developed for real applications due to lack of data privacy and security.
- Finally, some works such as [14, 22] have ignored uncertainty modeling, while the intermittent nature of uncertain parameters has a significant impact on decision making process of operators. Although uncertainty modeling has been considered in some of the existing works like [11, 13, 33], the utilized approaches are based on scenarios and probability distribution functions, which are time consuming and complex to tackle with.

Table 1 compare the proposed model and the literature reviewed earlier. This paper presents a robust decentralized energy management of interconnected MGs based on power, heat, and hydrogen, considering electricity price uncertainty. RO is selected to conduct the uncertainties. Additionally, in the presented framework, thermal and electrical DR programs are used to manage the energy consumption of customers. Power to heat (P2H) and $P2H_2$ technologies and energy storage systems are utilized in the proposed MGs to increase system efficiency. Furthermore, HRSs and electrical vehicle parking lots (EVPLs) are deployed into the proposed MGs to satisfy the demand for hydrogen and power in the transportation sector. The main contributions of this work are highlighted as follows:

- A novel structure for MMGs based on power, heat, and hydrogen is proposed to meet the demands of heat, power, and hydrogen in the presence of HRSs and EVPLs.
- Power-to X technologies such as $P2H_2$ and P2H, along with multi-energy storage and thermal and electrical price-based demand response programs, are embedded in the proposed model to increase the overall efficiency of the MMGs.
- A decentralized energy management approach is introduced to control a set of interconnected developed MEMGs based on hydrogen, heat, and power. The ADMM algorithm is also used to decentralize the proposed model and preserve the privacy of MEMGs.
- A robust decentralized optimization method is proposed to deal with the uncertainty of electricity market price in the optimal scheduling problem of the MMG system.

Table 1. Comparison of the proposed model with the previous studies

Refs	Multi-microgrids	Energy carriers	Control approach		Decentralized algorithm	EVPL	HRS	P2X technologies		Uncertainty modeling
			Centralized	Decentralized				$P2H_2$	P2H	
[19]	✓	Power	×	✓	a novel AOP-looped CCG	×	×	×	×	RO/Stochastic
[11]	✓	Power and heat	✓	×	×	×	×	×	×	Stochastic
[20]	✓	Power	×	✓	Modified CCG and	×	×	×	×	Distributional robust model

					ADMM					predictive control
[14]	✓	Power	×	✓	Benders decomposition	×	×	×	×	Deterministic
[15]	✓	Power	✓	×	×	×	×	×	×	RO
[16]	✓	Power	×	✓	ADMM	×	×	×	×	RO
[13]	✓	Power	✓	×	×	×	×	×	×	Chance-constrained programming
[18]	✓	Power	×	✓	ATC	×	×	×	×	RO
[5]	×	Power, heating, cooling, and hydrogen	×	×	×	×	×	✓	×	Hybrid robust-stochastic
[27]	×	Power and hydrogen	×	×	×	×	✓	×	×	Distributed robust optimization approach
[22]	×	Power, heat, and cooling	×	×	×	×	×	×	✓	Deterministic
[31]	×	Power and hydrogen	×	×	×	×	✓	✓	×	Robust min-max model predictive control scheme
[33]	×	Power	×	×	×	✓	×	×	×	Stochastic
Proposed model	✓	Power, heat and hydrogen	×	✓	ADMM	✓	✓	✓	✓	RO

The rest of the article is categorized as follows: section 2 presents the problem description. Problem formulations are provided in section 3. Section 4 discusses case studies and simulation results in depth. Finally, the conclusions are presented in section 5.

2. Problem description

In this section, the MMG system structure and the proposed energy management model are described in detail. The proposed MMG system consists of four MEMGs, and each of the MEMGs is based on power, heat, and hydrogen, as depicted in Fig. 1. Multi-energy demands of MEMGs, i.e., electrical, thermal and hydrogen, are satisfied via MGs' generation components and multi-energy markets. Electrical and gas boilers, CHP unit, hydrogen to power (H2P) technology, renewable generations (Photovoltaic modules and wind turbines), energy storage systems (electrical, thermal, and hydrogen storages), thermal and electrical load, EVs, and HFCVs are employed in each MEMG as demonstrated in Fig. 1. Also, the $P2H_2$ technology, which consists of an AC/DC converter, an electrolyzer, and a compressor, is utilized as a pivotal component to convert electricity into hydrogen in each MEMG in a sufficient manner. HRS in the

proposed model is installed to provide the hydrogen demand for HFCVs in the transportation sector. The hydrogen provider company (HPC) can cover hydrogen deficiency. To transfer the required hydrogen, several methods such as hydrogen pipelines, hydrogen tube trailers, and natural gas network can be applied [35]. Since transmission of hydrogen through hydrogen pipelines imposes high costs and also supplying hydrogen into the natural gas network has a limitation (up to 5% is possible); thus, hydrogen tube trailers is a viable transportation option that could be used to integrate the HPC to energy systems [36]. This integration boosts renewable resources used in energy systems and contributes to climate change mitigation since producing hydrogen using renewables is considered as green hydrogen. Moreover, EVPLs are used to meet the demand of electric vehicles if necessary and to inject electricity into the grid when power generation is low.

An appropriate energy management system is needed once the modelling of MEMGs is done. There are two main energy management models in interconnected MEMGs, and those are centralized energy management and decentralized energy management. In the centralized model, MEMGs send information to a single energy management system which means if a problem occurs in the energy management system, the whole system gets affected. On the other hand, in the decentralized model, each MEMG is separately scheduled by itself, and each MEMGS are not informed of other MEMGs. Even though both models can be used to control interconnected MEMGs, in this proposed MMG system, a decentralized model is used for energy management. Fig. 1 exhibits the proposed energy management of the MMG system. As shown in the figure, a coordinator manages information and energy exchange between MEMGs and the multi-energy market. After considering the domestic resources, energy prices, and local loads, each MEMG determines its optimal energy management in its control center. This model preserves privacy for each MEMG and decreases the total computational time for energy management of the MMG system.

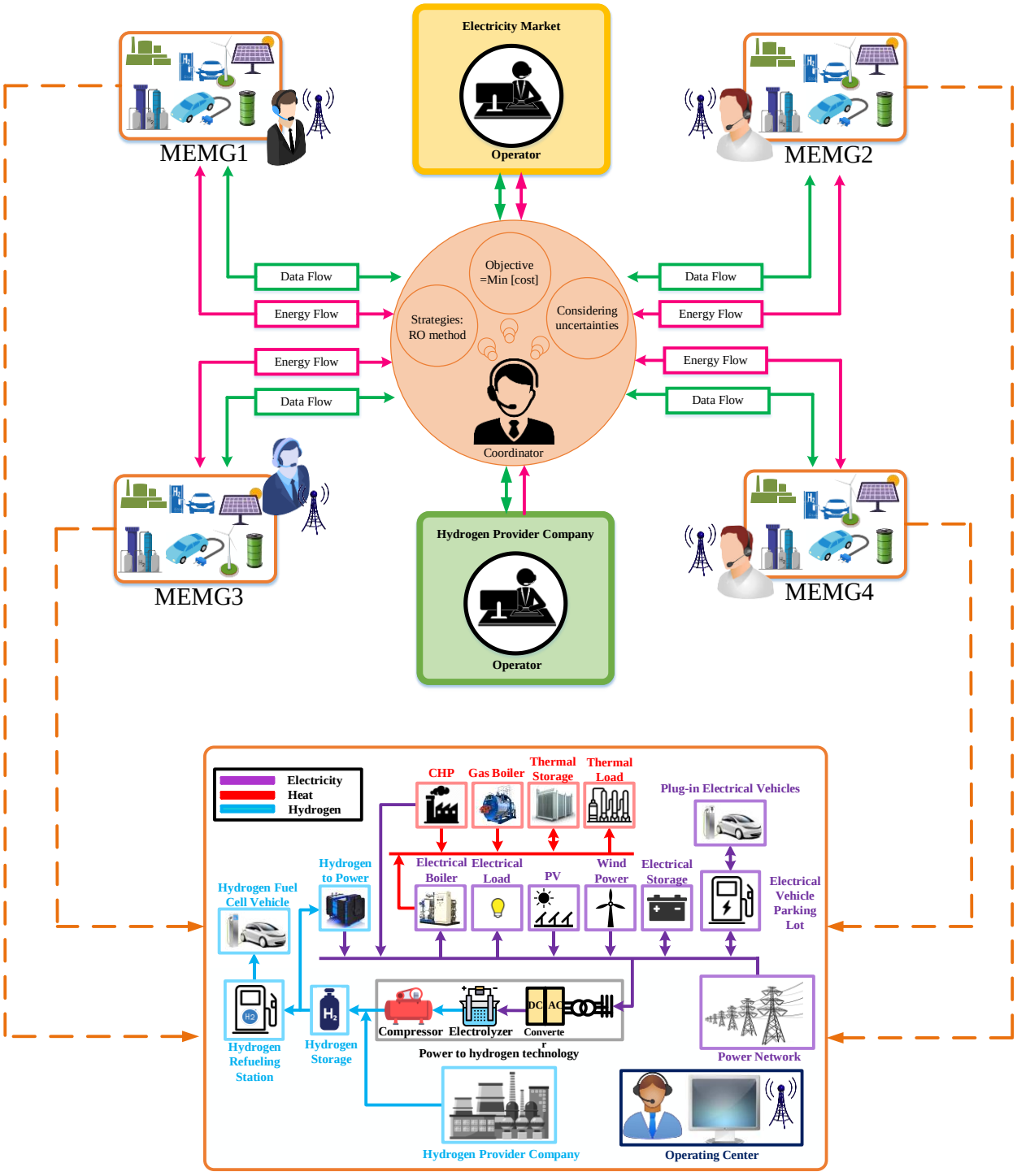

Fig. 1. The proposed structure of the MMG system

3. Centralized problem formulation under the deterministic model

3.1. Objective function

The objective function of this work is the total cost minimization of the MMG system scheduling problem. This objective function consists of three terms, and the first and second terms represent the exchanged cash flow between the coordinator and electricity and hydrogen provider company, while the third term expresses the operation costs of CHP units and boilers.

$$min \sum_{t=1}^{Nt} \left[\lambda_t^{el} P_t^{EM-Co} + \lambda_t^{hd} H_t^{EM-Co} + \sum_{m=1}^{Nm} \left[C_{t,m}^{chp} + C_{t,m}^{bo} \right] \right] \quad (1)$$

Equation (2) represents the operation cost of a CHP unit. The start-up and shut-down status of the CHP units are modeled as expressed in (3) and (4), respectively. Equation (5) implies that the cost of a CHP unit is determined by adding start-up and shut-down costs to the operation cost. Also, the quadratic generation cost of the boiler is given in (6).

$$C_{t,m}^{opr} = a_m \times (P_{t,m}^{chp})^2 + b_m \times P_{t,m}^{chp} + c_m + d_m \times (T_{t,m}^{chp})^2 + e_m \times T_{t,m}^{chp} + f_m \times (P_{t,m}^{chp} \times T_{t,m}^{chp}) \quad (2)$$

$$SU_{t,m}^{chp} \geq SUC_m \left[V_{t,m}^{chp} - V_{t-1,m}^{chp} \right] \quad ; \quad \forall i,t \quad (3)$$

$$SD_{t,m}^{chp} \geq SDC_m \left[V_{t-1,m}^{chp} - V_{t,m}^{chp} \right] \quad ; \quad \forall i,t \quad (4)$$

$$C_{t,m}^{chp} = C_{t,m}^{opr} + C_m^{su} \times SU_{t,m}^{chp} + C_m^{sd} \times SD_{t,m}^{chp} \quad (5)$$

$$C_{t,m}^{bo} = \alpha_m \times (T_{t,m}^{bo})^2 + \beta_m \times T_{t,m}^{bo} + \gamma_m \quad (6)$$

3.2. CHP units

The dual dependency of thermal energy and electricity generation of CHP units is considered in this work. To model this mutual dependency, a feasible operation region (FOR) is used. Two types of CHP units with convex and non-convex FORs are modeled in this work. Fig. 2 demonstrates the FOR of CHP units.

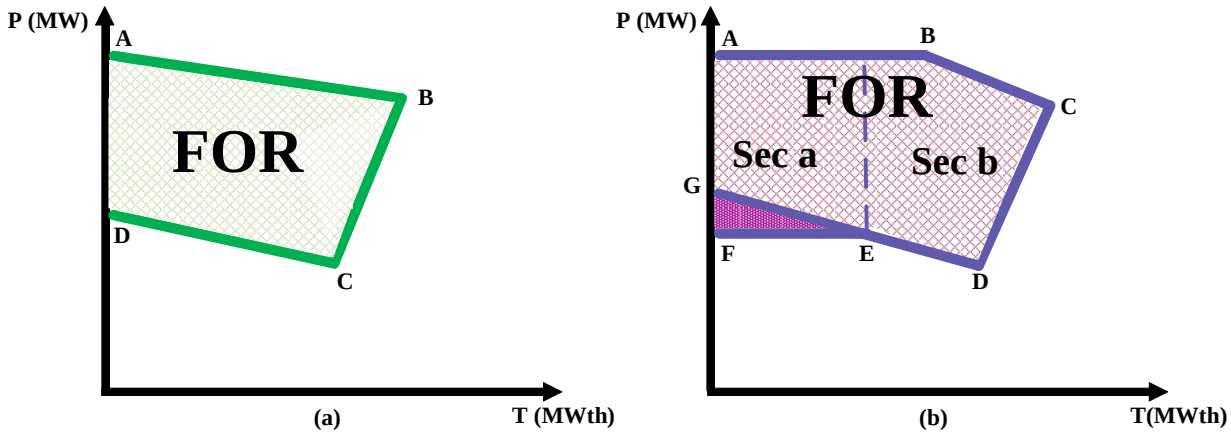

Fig. 2. Convex and non-convex FOR of CHP units

Equations (7)-(11) model the first type of CHP unit with the convex FOR. The region under the line AB is formulated in (7). The upper region of lines BC and CD are introduced in (8) and (9), respectively, where M represents a sufficient large number. Also, $V_{t,m}^{chp}=0$ means that the output power of CHP unit would be zero as represented in (8) and (9). In addition, the constraints associated with maximum electrical and thermal energy output of CHP units are modeled by (10) and (11), respectively.

$$P_{t,m}^{chp}-P_{m,A}^{chp}-\frac{P_{m,A}^{chp}-P_{m,B}^{chp}}{T_{m,A}^{chp}-T_{m,B}^{chp}}\left[T_{t,m}^{chp}-T_{m,A}^{chp}\right]\le 0 \tag{7}$$

$$P_{t,m}^{chp}-P_{m,B}^{chp}-\frac{P_{m,B}^{chp}-P_{m,C}^{chp}}{T_{m,B}^{chp}-T_{m,C}^{chp}}\left[T_{t,m}^{chp}-T_{m,B}^{chp}\right]\ge -\left[1-V_{t,m}^{chp}\right]\times M \tag{8}$$

$$P_{t,m}^{chp}-P_{m,C}^{chp}-\frac{P_{m,C}^{chp}-P_{m,D}^{chp}}{T_{m,C}^{chp}-T_{m,D}^{chp}}\left[T_{t,m}^{chp}-T_{m,C}^{chp}\right]\ge -\left[1-V_{t,m}^{chp}\right]\times M \tag{9}$$

$$0\le P_{t,m}^{chp}\le P_{m,A}^{chp}\times V_{t,m}^{chp} \tag{10}$$

$$0\le T_{t,m}^{chp}\le T_{m,B}^{chp}\times V_{t,m}^{chp} \tag{11}$$

Equations (12)-(20) represents the model of the CHP unit with non-convex FOR. The traditional formulation of the CHP with convex FOR cannot be implemented for this type of CHP unit. Hence, two binary variables $X_{t,a}$ and $X_{t,b}$ are implemented in the formulation of the CHP unit with non-convex

FOR. Therefore, the FOR of this type of CHP unit could be divided into two convex sub-regions a and b as indicated in Fig. 3. The region under the line BC is presented in (12). The upper region of the line CD is given by (13). Equations (14) and (15) formulate the regions over the lines EF and DE, respectively. Also, the electricity and heat output limitation of CHP units are described in (16) and (17), respectively. The binary variables $X_{t,a}$ and $X_{t,b}$ are implemented in (18)-(20) for specifying the operation point of CHP unit. Equation (18) states that the operation region of a committed CHP unit would be either a $(X_{t,a}=1)$ or b $(X_{t,b}=1)$.

$$P_{t,m}^{chp}-P_{m,B}^{chp}-\frac{P_{m,B}^{chp}-P_{m,C}^{chp}}{T_{m,B}^{chp}-T_{m,C}^{chp}}\left[T_{t,m}^{chp}-T_{m,B}^{chp}\right]\le 0 \tag{12}$$

$$P_{t,m}^{chp}-P_{m,C}^{chp}-\frac{P_{m,C}^{chp}-P_{m,D}^{chp}}{T_{m,C}^{chp}-T_{m,D}^{chp}}\left[T_{t,m}^{chp}-T_{m,C}^{chp}\right]\ge 0 \tag{13}$$

$$P_{t,m}^{chp}-P_{m,E}^{chp}-\frac{P_{m,E}^{chp}-P_{m,F}^{chp}}{T_{m,E}^{chp}-T_{m,F}^{chp}}\left[T_{t,m}^{chp}-T_{m,E}^{chp}\right]\ge -\left[1-X_{a,t}\right]\times M \tag{14}$$

$$P_{t,m}^{chp}-P_{m,D}^{chp}-\frac{P_{m,D}^{chp}-P_{m,E}^{chp}}{T_{m,D}^{chp}-T_{m,E}^{chp}}\left[T_{t,m}^{chp}-T_{m,D}^{chp}\right]\ge -\left[1-X_{b,t}\right]\times M \tag{15}$$

$$0\le P_{t,m}^{chp}\le P_{m,A}^{chp}\times V_{t,m}^{chp} \tag{16}$$

$$0\le T_{t,m}^{chp}\le T_{m,C}^{chp}\times V_{t,m}^{chp} \tag{17}$$

$$X_{a,t}+X_{b,t}=V_{t,m}^{chp} \tag{18}$$

$$T_{t,m}^{chp}-T_{m,E}^{chp}\le\left[1-X_{a,t,m}\right]\times M \tag{19}$$

$$T_{t,m}^{chp}-T_{m,E}^{chp}\ge -\left[1-X_{b,t,m}\right]\times M \tag{20}$$

3.3. Gas boiler

Gas boiler is used along with a CHP unit and a P2H system for supplying domestic heat demand of each MEMG. The constraint related to output power generation of gas boiler is given in (21).

$$0 \le T_{t,m}^{bo} \le T_{m}^{bo,\max} \tag{21}$$

3.4. Power to heat technology

A P2H facility would be installed if gas boiler, CHP unit, and thermal storage cannot satisfy heat load or when their operation is not economical. The P2H converts electricity into thermal energy as described in (22). Also, equation (23) limits the converted heat by the P2H technology.

$$T_{t,m}^{P2H} = \eta_{m}^{P2H} P_{t,m}^{P2H} \tag{22}$$

$$0 \le T_{t,m}^{P2H} \le T_{m}^{P2H,\max} \tag{23}$$

3.5. Electrical storage

In each MEMG, energy storages systems are operated to increase the efficiency of the MMG system. Equation (24) determines the amount of stored electricity in the electrical storage system (ESS). Equations (25)-(27) are stated for limiting the level of stored electricity, charging power, and discharging power, respectively. Equation (28) ensures that the storage system does not work in charging and discharging modes simultaneously. As presented in equation (29), the equality of the initial and final power level of the ESS is ensured.

$$SoC_{t,m}^{ES} = SoC_{t-1,m}^{ES} + \eta_{m}^{ch,ES} \times P_{t,m}^{ch,ES} - \frac{P_{t,m}^{disch,ES}}{\eta_{m}^{disch,ES}} \tag{24}$$

$$SoC_{m}^{\min,ES} \le SoC_{t,m}^{ES} \le SoC_{m}^{\max,ES} \tag{25}$$

$$\underline{P}_{m}^{ch,ES} I_{t,m}^{ch,ES} \le P_{t,m}^{ch,ES} \le \overline{P}_{m}^{ch,ES} I_{t,m}^{ch,ES} \tag{26}$$

$$\underline{P}_{m}^{disch,ES} I_{t,m}^{disch,ES} \le P_{t,m}^{disch,ES} \le \overline{P}_{m}^{disch,ES} I_{t,m}^{disch,ES} \tag{27}$$

$$I_{t,m}^{ch,ES} + I_{t,m}^{disch,ES} \le 1 \tag{28}$$

$$SoC_{(t=0),m}^{ES} = SoC_{(t=Nt),m}^{ES} \tag{29}$$

3.6. Thermal storage

Operational constraints related to thermal storages are represented in (30) to (35). The heat level of the thermal storage system (TSS) at each hour is presented in (30). Equation (31) represents the capacity limitation of the TSS. Similar to the ESS, charging and discharging limitations of the TSS are constrained in (32) and (33), respectively. In addition, equation (34) states that the TSS operates in one of the discharging or charging statuses. Equation (35) ensures that the initial and final quantity of stored thermal energy in the TSS are equal.

$$SoC_{t,m}^{TS} = SoC_{t-1,m}^{TS} + \eta_m^{ch,TS} \times P_{t,m}^{ch,TS} - \frac{P_{t,m}^{disch,TS}}{\eta_m^{disch,TS}} \tag{30}$$

$$SoC_m^{\min,TS} \le SoC_{t,m}^{TS} \le SoC_m^{\max,TS} \tag{31}$$

$$\underline{T}_m^{ch,TS} I_{t,m}^{ch,TS} \le T_{t,m}^{ch,TS} \le \overline{T}_m^{ch,TS} I_{t,m}^{ch,TS} \tag{32}$$

$$\underline{T}_m^{disch,TS} I_{t,m}^{disch,TS} \le T_{t,m}^{disch,TS} \le \overline{T}_m^{disch,TS} I_{t,m}^{disch,TS} \tag{33}$$

$$I_{t,m}^{ch,TS} + I_{t,m}^{disch,TS} \le 1 \tag{34}$$

$$SoC_{(t=0),m}^{TS} = SoC_{(t=Nt),m}^{TS} \tag{35}$$

3.7. Power to hydrogen technology

$P2H_2$ technology converts electricity into hydrogen via the electrolysis process, as described in (36). Moreover, the limitations related to the power consumption of $P2H_2$ technology is specified in (37).

$$H_{t,m}^{P2H_2} = \eta_m^{P2H_2} P_{t,m}^{P2H_2} \tag{36}$$

$$0 \le P_{t,m}^{P2H_2} \le P_m^{P2H_2,\max} \tag{37}$$

3.8. Hydrogen storage

Operational constraints associated with hydrogen storages are represented from (38) to (43). Equation (38) represents the dynamic model of the hydrogen storage system (HSS). The quantity of stored hydrogen in the HSS is limited as (39). Also, limitations related to charging and discharging of the HSS are stated in (40) and (41), respectively. Equation (42) is presented in order to ensure the operation of the

HSS in one of the charging or discharging modes. In addition, the quantity of stored hydrogen in the HSS must be the same at the initial and final hour of the scheduling cycle, as described in (43).

$$SoC_{t,m}^{HS} = SoC_{t-1,m}^{HS} + \eta_m^{ch,HS} \times H_{t,m}^{ch,HS} - \frac{H_{t,m}^{disch,HS}}{\eta_m^{disch,HS}} \quad (38)$$

$$SoC_m^{\min,HS} \le SoC_{t,m}^{HS} \le SoC_m^{\max,HS} \quad (39)$$

$$\underline{H}_m^{ch,HS} I_{t,m}^{ch,HS} \le H_{t,m}^{ch,HS} \le \bar{H}_m^{ch,HS} I_{t,m}^{ch,HS} \quad (40)$$

$$\underline{H}_m^{disch,HS} I_{t,m}^{disch,HS} \le H_{t,m}^{disch,HS} \le \bar{H}_m^{disch,HS} I_{t,m}^{disch,HS} \quad (41)$$

$$I_{t,m}^{ch,HS} + I_{t,m}^{disch,HS} \le 1 \quad (42)$$

$$SoC_{(t=0),m}^{HS} = SoC_{(t=Nt),m}^{HS} \quad (43)$$

3.9. Electrical vehicle parking lot

EVPL operators enable EVs to join the power market via both vehicles to grid (V2G) and Grid to Vehicles (G2V) statuses. Equation (44) calculates the available energy of EVs at each hour. The storage capacity, G2V power, and V2G power of EVs which are parked in each EVPL are limited by (45)-(47), respectively. Moreover, equation (48) is used to avoid simultaneous V2G and G2V statuses. Also, as explained in equation (49) when EVs leave the EVPL, their batteries must be fully charged. Additionally, the initial SoC of the EVs should be determined according to their energy levels at the arrival time, which is stated by (50). It should be noted that the total storage capacity of an EVPL is affected by the departure/arrival of EVs from/to it.

$$SoC_{t,m,j,k}^{EV} = SoC_{t-1,m,j,k}^{EV} + \eta_{m,j}^{ch,EV} \times P_{t,m,j,k}^{ch,EV} - \frac{P_{t,m,j,k}^{disch,EV}}{\eta_{m,j}^{disch,EV}} \quad (44)$$

$$SoC_{m,j}^{EV,\min} \le SoC_{m,t,j,k}^{EV} \le SoC_{m,j}^{EV,\max} \quad (45)$$

$$\underline{P}_{m,j}^{ch,EV} I_{m,t,j,k}^{ch,EV} \le P_{m,t,j,k}^{ch,EV} \le \bar{P}_{m,j}^{ch,EV} I_{m,t,j,k}^{ch,EV}; \forall t \in [t_{arv}, t_{dep}] \quad (46)$$

$$\underline{P}_{m,j}^{disch,EV} I_{m,t,j,k}^{disch,EV} \le P_{m,t,j,k}^{disch,EV} \le \bar{P}_{m,j}^{disch,EV} I_{m,t,j,k}^{disch,EV}; \forall t \in [t_{arv}, t_{dep}] \quad (47)$$

$$I_{m,t,j}^{ch,EV} + I_{m,t,j}^{disch,EV} \le 1; \forall t \in [t_{arv}, t_{dep}] \quad (48)$$

$$SoC_{m,t_{dep},j,k}^{EV} = SoC_{m,j}^{EV,\max} \quad (49)$$

$$SoC_{m,t_{arv},j,k}^{EV} = SoC_{m,j}^{EV,\min} \quad (50)$$

3.10. Hydrogen refueling station

HRSs are installed to supply the hydrogen demand of HFCVs. Entry time, departure time, and traveling plan of HFCVs are considered as private information in this study. Although in a few studies, HFCVs are taken as an entity that are controlled by an aggregator, in reality, not all HFCVs would like to be controlled [27]. Therefore, the hydrogen demand of HFCVs is assumed to be directly forecasted by HRSs based on their historical data as shown in (51).

$$H_{t,m}^{load} = H_{t,m}^{HRS} \quad (51)$$

3.11. Hydrogen to power

The amount of hydrogen consumed by H2P technology with regard to its generated electricity is expressed by (52). Moreover, the consumed hydrogen limitation as well as limitations related to power generation of H2P at each hour of the scheduling horizon is stated by (53) and (54), respectively.

$$H_{t,m}^{H2P} = \frac{P_{t,m}^{H2P}}{\eta_m^{H2P} LHV_m} \quad (52)$$

$$\underline{H}_m^{H2P} \le H_{t,m}^{H2P} \le \bar{H}_m^{H2P} \quad (53)$$

$$\underline{P}_m^{H2P} \le P_{t,m}^{H2P} \le \bar{P}_m^{H2P} \quad (54)$$

3.12. Renewable generations

PV panels and WTs are studied in the proposed MMG system as renewable energy sources for clean energy procurement. Equation (55) formulates the available electricity produced by WTs. Also, PV output is related to its characteristics and environmental conditions, as shown in (56)-(60).

$$P_{t,m}^{WT} = N_m^{WT} \times \begin{Bmatrix} 0 & v_t < v_{in}^c \\ P_{rated}^{WT} \times \left(\frac{v_t - v_{in}^c}{v_{rated} < v_{in}^c} \right)^3 & v_{in}^c \le v_t < v_{rated} \\ P_{rated}^{WT} & v_{rated} \le v_t < v_{out}^c \\ 0 & v_{out}^c \le v_t \end{Bmatrix} \quad (55)$$

$$Tc_t = AT_t + sor_t \times \left(\frac{N_{OT} - 20}{0.8} \right) \quad (56)$$

$$I_t = sor_t \times [I_{sc} + K_i \times (Tc_t - 25)] \quad (57)$$

$$V_t = V_{OC} - K_v \times Tc_t \quad (58)$$

$$FF = \frac{V_{MPP} \times I_{MPP}}{V_{OC} \times I_{SC}} \quad (59)$$

$$P_{t,m}^{PV} = N_M^{PV} \times FF \times V_t \times I_t \quad (60)$$

3.13. Demand response programs

Demand management programs make it possible for generation companies and their customers to achieve economic benefits by managing energy consumption. In this paper, the electrical and thermal energy consumers of the MMG system are stimulated to manage their usage by implementing price-based demand response programs. The constraints associated with the electrical DR program are given by (61)-(64). Equation (61) determines the new electrical load after considering the electrical DR program. The limitation of the electrical load increment, as stated in (62). Moreover, the decrease of the electrical load is limited, as presented in (63). According to equation (64), the total increased and curtailed loads must be equal at the end of the day. Identical to the electrical DR program, the constraints related to the thermal DR program are expressed by (65) to (68).

$$P_{t,m}^{load,EDR} = P_{t,m}^{load} + P_{t,m}^{inc} - P_{t,m}^{curt} \quad (61)$$

$$0 \le P_{t,m}^{inc} \le D_m^{inc} \times \bar{P}_m^{inc} \quad (62)$$

$$0 \le P_{t,m}^{curt} \le D_m^{curt} \times \bar{P}_m^{curt} \tag{63}$$

$$\sum_{m=1}^{Nt} P_{t,m}^{inc} = \sum_{m=1}^{Nt} P_{t,m}^{curt} \tag{64}$$

$$T_{t,m}^{load,TDR} = T_{t,m}^{load} + T_{t,m}^{inc} - T_{t,m}^{curt} \tag{65}$$

$$0 \le T_{t,m}^{inc} \le D_m^{inc} \times \bar{T}_m^{inc} \tag{66}$$

$$0 \le T_{t,m}^{curt} \le D_m^{curt} \times \bar{T}_m^{curt} \tag{67}$$

$$\sum_{t=1}^{Nt} T_{t,m}^{inc} = \sum_{t=1}^{Nt} T_{t,m}^{curt} \tag{68}$$

3.14. Energy balance

Equations associated with electricity balance are shown below by (69)-(71). The thermal energy balance is described in (72). In addition, the equations related to hydrogen balance are stated in (73)-(75). It should be noted that the coordinator does not sell hydrogen to the HPC which means that hydrogen is exchanged between MEMGs and the HPC through buying hydrogen from HPC when needed as implied in (74).

$$\begin{aligned} P_{t,m}^{MEMG-Co} &= P_{t,m}^{chp} - P_{t,m}^{P2H} + P_{t,m}^{disch} - P_{t,m}^{ch} - P_{t,m}^{P2H_2} \\ &+ \sum_{j=1}^{Nj} \sum_{k=1}^{Nk} N_m^{EV} R_k Q_j (-P_{t,m,j,k}^{ch,EV} + P_{t,m,j,k}^{disch,EV}) + P_{t,m}^{H2P} + P_{t,m}^{PV} + P_{t,m}^{WT} - P_{t,m}^{load,EDR} \end{aligned} \tag{69}$$

$$P_{t,m}^{MEMG-Co} + P_{t,m}^{Co-MEMG} = 0 \tag{70}$$

$$\sum_{m=1}^{Nm} P_{t,m}^{Co-MEMG} = P_t^{EM-Co} \tag{71}$$

$$\sum_{m=1}^{Nm} \left[T_{t,m}^{chp} + T_{t,m}^{bo} + T_{t,m}^{P2H} + T_{t,m}^{disch} - T_{t,m}^{ch} - T_{t,m}^{load,TDR} \right] = 0 \tag{72}$$

$$H_{t,m}^{MEMG-Co} = H_{t,m}^{H2P} + H_{t,m}^{HRS} - H_{t,m}^{P2H_2} \tag{73}$$

$$H_{t,m}^{MEMG-Co} - H_{t,m}^{Co-MEMG} = 0 \tag{74}$$

$$\sum_{m=1}^{Nm} H_{t,m}^{Co-MEMG} = H_t^{EM-Co} \quad (75)$$

4. *Decentralized problem formulation under the robust optimization*

4.1 Robust optimization

In this paper, multiple parameters including power market price, wind power output, PV power output and various demands can be considered as uncertainty. However, only power market price intermittency has been relieved through the robust optimization on the ground that it has the foremost influence on the decision-making process and its impact dwarf other uncertainties [37-39]. In addition, since the coordinator is the only eligible entity to participate in the power market and act as a link between the power market and microgrids, the uncertainty of the power market has a direct impact on its decisions and consequently incurred operation costs. So, in the current work, power market uncertainty has priority to other uncertain parameters to be taken into consideration. In the proposed model, the robust optimization (RO) method is used to handle the uncertainty concerns with power market price. RO approach considers the worst-case situation of the electricity market price in order to obtain the optimal solution for the scheduling problem of the MMG system [5]. Moreover, the robustness of the scheduling problem is controlled by using an integer parameter Γ known as uncertainty budget. The uncertainty budget is a known parameter that can be selected from the range [0: Nt]. The value of this parameter determines the amount of risk that the coordinator wants to take. For instance, Γ=0 means no uncertainty has been considered and Γ=24 indicates that uncertainty has been taken into consideration for all hours (24 hours). In doing so, the robust optimization method has been run for a specific amount of Γ, then the worst-case uncertain hours have been determined via the optimization. In other words, the uncertainty budget is a controllable parameter that provides authority for the coordinator to make a decision on how much risk it wants to take

for the scheduling of the next 24 hours. Based on this parameter, the coordinator can take a risk-neutral or risk-averse manner. Considering ε as the deviation of the market price, the objective function could be restated as follows:

$$\min \sum_{t=1}^{Nt} \left[\lambda_t^{hd} H_t^{EM-Co} + \sum_{m=1}^{Nm} \left[C_{t,m}^{chp} + C_{t,m}^{bo} \right] + \lambda_t^{el} P_t^{EM-Co} + \underbrace{\max_{\{k|k\subseteq Nt, |k|\le\Gamma\}} \sum_{t\in k} \varepsilon \left| P_t^{EM-Co} \right|}_{\varphi} \right] \quad (76)$$

Due to the min-max model of the objective function, the worst-case scenario is provided for the power price by the inner term of the objective function while the outer term of the objective function is minimized. Since there is a condition on the max term if the Eq. (76) causes computational burden, they are reformulated as equations (77)-(79) and the condition could be relaxed using an auxiliary variable, i.e., *z*, and two constraints [40, 41]. Furthermore, in equation (77) $\varepsilon \left| P_t^{EM-Co} \right|$ can be defined as a penalty term concerns with real-time power market to mitigate its deviations. Maximization of this relation leads to find the worst-case scenario in real-time prices.

$$\varphi = \max \sum_{t\in Nt} \varepsilon \left| P_t^{EM-Co} \right| z_t \quad (77)$$

$$\sum_{t\in Nt} z_t \le \Gamma \ : \alpha \quad (78)$$

$$0 \le z_t \le 1, \ \forall t \in Nt \ : \beta \quad (79)$$

In doing so, the max term of Eq. (76) has been restated in a simple way, yet Eq. (76) stills a min-max problem. In order to reformulate (77)-(79) into a min problem as (80)-(85), the duality theory is applied [42]. Therefore, the complex min-max problem is changed into a linear minimization problem which is much easier to solve with conventional solvers. It should be mentioned that α, β_t denote dual variables and y_t is an auxiliary variable in the following equations.

$$\varphi = \min \left[\sum_{t=1}^{Nt} \beta_t + \alpha \Gamma \right] \quad (80)$$

$$\alpha + \beta_t \geq \varepsilon\, y_t \tag{81}$$

$$\beta_t \geq 0 \tag{82}$$

$$\alpha \geq 0 \tag{83}$$

$$y_t \geq 0 \tag{84}$$

$$-y_t \leq P_t^{EM-Co} \leq y_t \tag{85}$$

The achieved robust optimization problem is stated as follows. It is noteworthy that, $\lambda_t^{hd}, \lambda_t^{el}$ are hydrogen and electricity prices, Γ is the uncertainty budget and ε is the allowed price deviation, which all of these symbols refer to pre-defined parameters. Hence, the robust optimization problem of (89)-(92) is a mixed-integer linear programming.

$$\min \sum_{t=1}^{Nt}\left[\lambda_t^{hd} H_t^{EM-Co} + \sum_{m=1}^{Nm}\left[C_{t,m}^{chp} + C_{t,m}^{bo}\right]_t\right] + \sum_{t=1}^{Nt}\left[\lambda_t^{el} P_t^{EM-Co} + \beta_t\right] + \alpha\,\Gamma \tag{86}$$

$$\alpha + \beta_t \geq \varepsilon\, y_t \tag{87}$$

$$\beta_t \geq 0 \tag{88}$$

$$\alpha \geq 0 \tag{89}$$

$$y_t \geq 0 \tag{90}$$

$$-y_t \leq P_t^{EM-Co} \leq y_t \tag{91}$$

(2)-(75) (92)

4.2. ADMM algorithm

Centralized and decentralized energy platforms are two popular approaches for energy management of MMG systems. Both centralized and decentralized energy platforms have their own merits and demerits. Regarding a centralized system, since in a centralized system there is only one entity that operates the system, it is easy to implement and maintenance and any failure in the system could be detected easily. However, operation of centralized systems has a computational burden, it needs a lot of connectivity which causes a reduction of reliability, and

also it cannot be expanded. On the other hand, a decentralized system can be expanded easily and used in large-scale systems, also it can be run with low computational complexity, and finally, even more importantly, as each entity runs its optimization problem locally, there is no need for sharing data with a third party and this issue contributes to the cyber security of an energy system. But there exist minor pitfalls for a decentralized system. Firstly, it needs a bidirectional communication system and secondly, the convergence of this approach could be affected by communication network. All in all, the advantages of a decentralized system outweigh not only its disadvantages but also the advantages of a centralized approach [43]. Therefore, decentralized approaches have been implemented in many studies in recent years. For example, in [44], an equivalent model-based non-iterative solution has been used in distributed operation of an integrated electricity and heat system. In [45], a non-iterative decoupled solution has been employed for robust scheduling of an integrated electricity and heat system. Also, a price-quantity decomposition (PQD) method along with warm-start strategies has been proposed for distributed operation of an integrated electricity and heat system in [46]. Most of the developed decomposition algorithms for dealing with complicating constraints are usually based on Lagrangian functions to relax the complicating constraints such as Lagrange decomposition (LD), ADMM, analytical target cascading theory (ATC), and PQD. Among these algorithms, the ADMM is a well-known and prevalent technique to be used in decomposition problems [38, 47]. Further, it can be easily applied to large-scale problems without affecting its convergence and computational complexity [48]. Therefore, in this paper, in order to decompose the proposed model, the ADMM is used as an iterative-based decentralized algorithm. The ADMM is known as a distributed convex optimization approach that provides convergence by using iterative local optimization for independent entities. When comparing with the centralized problem, using the ADMM for decentralizing, the scheduling problem not only ensures independence and privacy of different entities but also enhances the scalability of the proposed model by decreasing the computational time for energy management of the MMG system. Therefore, MEMGs and the coordinator, which are considered separate entities, can be operated in a decentralized manner by implementing the ADMM. In this regard, the augmented Lagrangian function can be written as below:

$$
\begin{aligned}
L(X,\varphi,\beta,\rho,\theta) &= \sum_{t=1}^{Nt}\sum_{m=1}^{Nm}\left[C_{t,m}^{chp}+C_{t,m}^{bo}\right]+\sum_{t=1}^{Nt}\left[\lambda_t^{hd}H_t^{EM-Co}+\lambda_t^{el}P_t^{EM-Co}+\beta_t\right]+\alpha\Gamma \\
&+\sum_{t=1}^{Nt}\sum_{m=1}^{Nm}\left[\varphi_{t,m}\left(P_{t,m}^{Co-MEMG}+P_{t,m}^{MEMG-Co}\right)\right]+\sum_{t=1}^{Nt}\sum_{m=1}^{Nm}\left[\frac{\rho}{2}\left\|P_{t,m}^{Co-MEMG}+P_{t,m}^{MEMG-Co}\right\|^2\right] \\
&+\sum_{t=1}^{Nt}\sum_{m=1}^{Nm}\left[\beta_{t,m}\left(H_{t,m}^{Co-MEMG}-H_{t,m}^{MEMG-Co}\right)\right]+\sum_{t=1}^{Nt}\sum_{m=1}^{Nm}\left[\frac{\theta}{2}\left\|H_{t,m}^{Co-MEMG}-H_{t,m}^{MEMG-Co}\right\|^2\right]
\end{aligned}
\tag{93}
$$

Where, X denotes decision variables; φ,β are dual variables and ρ,θ are penalty factors. In Eq. (93), all the complicated constraints (i.e., Eq. (70) and Eq. (74)) have been relaxed, and the optimization problem does not deal with any barrier to be decomposed anymore. By performing that, the local optimization problem for each entity, including each MEMG and the coordinator, can be extracted. Equation (94) describes the local optimization problem for each MEMG. Also, the optimization problem is solved by the coordinator, as stated in (95).

$$
\begin{aligned}
&Min\left[\sum_{t=1}^{Nt}\left[C_{t,m}^{chp}+C_{t,m}^{bo}\right]\right. \\
&+\sum_{t=1}^{Nt}\left[\varphi_{t,m}\left(\tilde{P}_{t,m}^{Co-MEMG}+P_{t,m}^{MEMG-Co}\right)\right]+\sum_{t=1}^{Nt}\left[\frac{\rho}{2}\left\|\tilde{P}_{t,m}^{Co-MEMG}+P_{t,m}^{MEMG-Co}\right\|^2\right] \\
&\left.+\sum_{t=1}^{Nt}\left[\beta_{t,m}\left(\tilde{H}_{t,m}^{Co-MEMG}-H_{t,m}^{MEMG-Co}\right)\right]+\sum_{t=1}^{Nt}\left[\frac{\theta}{2}\left\|\tilde{H}_{t,m}^{Co-MEMG}-H_{t,m}^{MEMG-Co}\right\|^2\right]\right]
\end{aligned}
\tag{94}
$$

$$
\begin{aligned}
&Min\left[\sum_{t=1}^{Nt}\left[\lambda_t^{hd}H_t^{EM-Co}+\lambda_t^{el}P_t^{EM-Co}+\beta_t\right]+\alpha\Gamma\right. \\
&+\sum_{t=1}^{Nt}\sum_{m=1}^{Nm}\left[\varphi_{t,m}\left(P_{t,m}^{Co-MEMG}+\tilde{P}_{t,m}^{MEMG-Co}\right)\right]+\sum_{t=1}^{Nt}\sum_{m=1}^{Nm}\left[\frac{\rho}{2}\left\|P_{t,m}^{Co-MEMG}+\tilde{P}_{t,m}^{MEMG-Co}\right\|^2\right] \\
&\left.+\sum_{t=1}^{Nt}\sum_{m=1}^{Nm}\left[\beta_{t,m}\left(H_{t,m}^{Co-MEMG}-\tilde{H}_{t,m}^{MEMG-Co}\right)\right]+\sum_{t=1}^{Nt}\sum_{m=1}^{Nm}\left[\frac{\theta}{2}\left\|H_{t,m}^{Co-MEMG}-\tilde{H}_{t,m}^{MEMG-Co}\right\|^2\right]\right]
\end{aligned}
\tag{95}
$$

The steps of the ADMM for decentralizing the proposed model is provided as follows:

Step 1) Initialization: All the initial values of required parameters including iteration index, convergence criteria, dual variables, penalty factors and initial values of fixed variables related to other entities are

initialized. These items are denoted as ν, ε, σ, φ, β, ρ, θ, $\tilde{P}_{t,m}^{Co-MEMG}$, $\tilde{P}_{t,m}^{MEMG-Co}$, $\tilde{H}_{t,m}^{Co-MEMG}$, $\tilde{H}_{t,m}^{MEMG-Co}$

Step 2) Solving local optimization problems: The local optimization problem for each MEMG in (94) and the coordinator in (95) are solved then the following fixed variables are updated: $\tilde{P}_{t,m}^{Co-MEMG}$, $\tilde{P}_{t,m}^{MEMG-Co}$, $\tilde{H}_{t,m}^{Co-MEMG}$, $\tilde{H}_{t,m}^{MEMG-Co}$.

Step 3) Updating dual variables: In this step, the dual variables are updated according to Eqs. (96)-(97) based on outputs of step 2.

$$\varphi_{t,m}^{(\nu)} = \varphi_{t,m}^{(\nu-1)} + \rho(P_{t,m}^{Co-MEMG,(\nu)} + P_{t,m}^{MEMG-Co,(\nu)}) \tag{96}$$

$$\beta_{t,m}^{(\nu)} = \beta_{t,m}^{(\nu-1)} + \theta(H_{t,m}^{Co-MEMG,(\nu)} - H_{t,m}^{MEMG-Co,(\nu)}) \tag{97}$$

Step 4) Checking the convergence criteria: After updating dual variables in the previous step, the convergence criteria are checked by relations (98)-(99) to recognize whether the existing errors are acceptable or not. If the criteria satisfy, the algorithm stop; otherwise, the algorithm continues from step 2 by updating the iteration index as $\nu \to \nu+1$.

$$\left| P_{t,m}^{Co-MEMG,(\nu)} + P_{t,m}^{MEMG-Co,(\nu)} \right| \le \varepsilon \tag{98}$$

$$\left| H_{t,m}^{Co-MEMG,(\nu)} - H_{t,m}^{MEMG-Co,(\nu)} \right| \le \sigma \tag{99}$$

5. Simulation results and discussion

The presented decentralized robust day-ahead energy management scheduling was rendered on an energy system composed of four MGs and a coordination center, as shown in Fig. 1. Each MG is equipped with a CHP unit; P2H, $P2H_2$ and H2P technologies; ESS, TSS, and HSS as energy storage systems; EV and HFCV; WT and PV panels as renewable energy sources. First, the operators of the MGs contact the coordinator center in order to submit their bids for power and hydrogen. After collecting bids, the

coordinators trades with the wholesale market to meet MGs demand. Fig. 4 shows the predicted wholesale power market prices for the next day.

Fig. 5 depicts the predicted day-ahead hydrogen demand for each MG. Hydrogen price is considered as 3.3 $/kg. The number of integrated electric vehicles for MGs 1 and 2 is 100 and for MGs 3 and 4 are 125. EVs have different arrival times, departure times and initial SoCs. To simulate the previous statement, 10 clusters are taken into account [49]. The MGs operator can shift up/down end-users' load by 10% to manage the demand side. Techno-economic characteristics of the CHP units and boilers are available in [50]. In addition, technical details of energy storage systems are introduced in Table 1. Owing to evaluate the wholesale power market uncertainty impact on the MGs scheduling, results are presented through two cases. In the first case, the system is evaluated in a deterministic manner and in the second case, robust optimization is included to manage the uncertainty. All the simulations were performed employing the SBB solver of the general algebraic modeling system (GAMS) software on a PC with Intel® Core™ i7-4710HQ CPU @ 2.5 GHz and 8GB RAM. Also, in terms of simulation and coding, the Discrete and Continuous Optimizer (DICOPT) solver in GAMS software. The DICOPT solver is a high-level and reliable solver that can solve even non-convex problems and its obtained results are globally optimal [51, 52]. Figure 3 presents a flowchart to show the DICOPT solver process with more details. Since the ADMM algorithm is based on augmented Lagrangian function and this function has a non-linear term due to $\|.\|^2$; therefore, after applying the ADMM, the centralized MILP optimization problem is converted to a MINLP problem. However, the DICOPT solver could efficiently handle any MINLP problem. First of all, an MINLP problem divided into NLP and MIP problems. The MIP master problem is solved via CPLEX solver, which is based on branch and cut method to achieve optimal solution [53], and the NLP part is solved by CONOPT solver. It is noteworthy that in solving process, binary variables are fixed and this issue alleviates concerns associated with binary variables [52]. In addition, there are two options namely "optca", which determines the absolute error of the global solver, and "optcr", which determines the relative error of the global solver. These two options can be adjusted to zero in order to minimize the

absolute and relative gaps and in doing so, not only does the running time is reduced but also deviations from centralized solutions are minimized [54, 55].

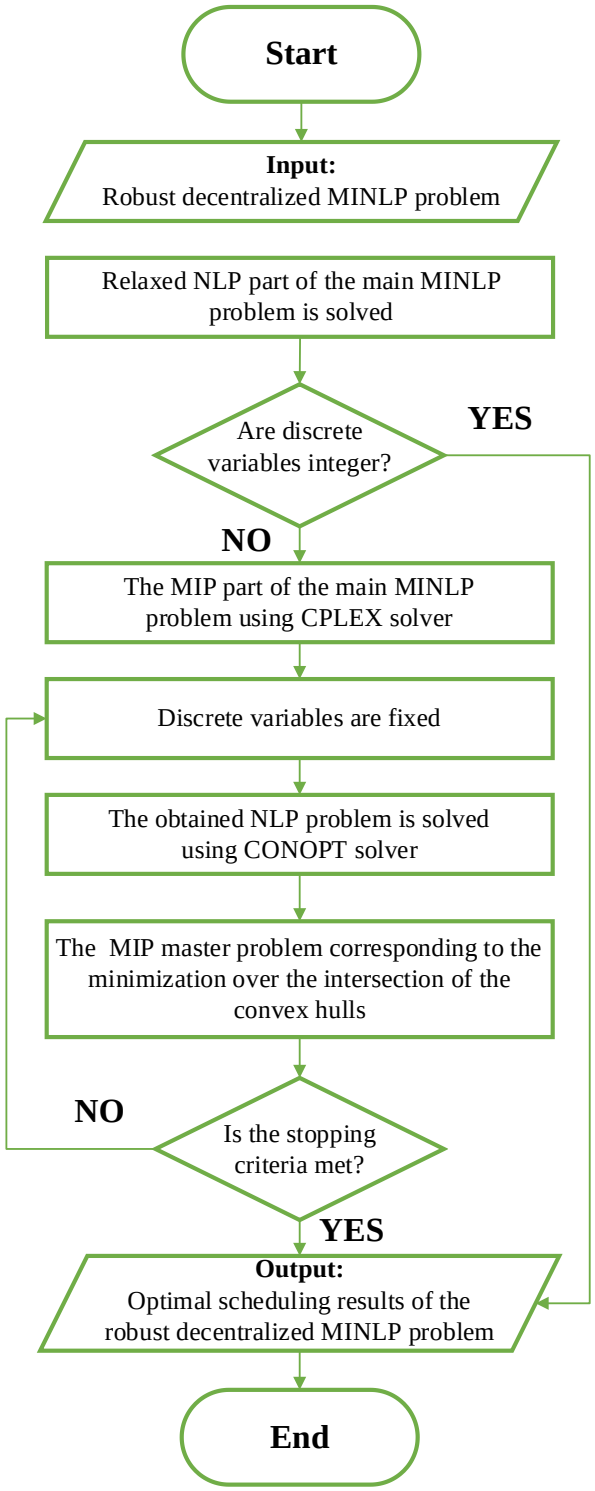

Fig. 3. The DICOPT algorithm for solving the robust decentralized MINLP problem

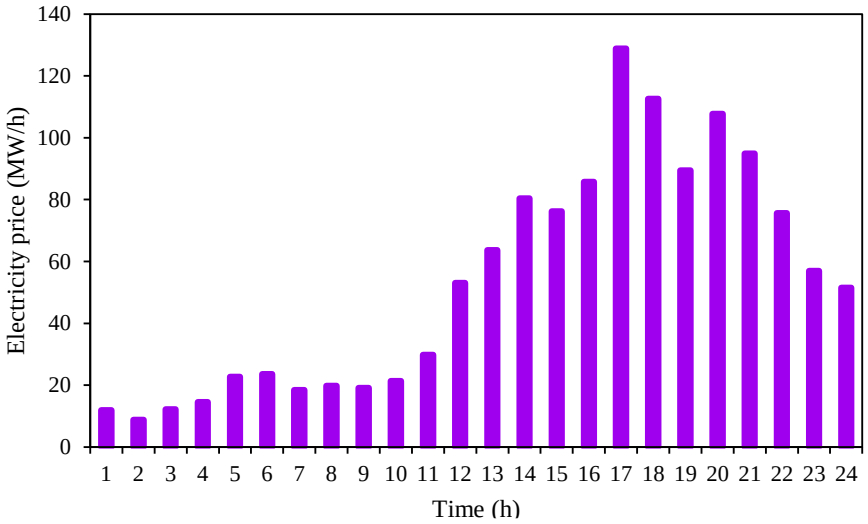

Fig. 4. Hourly predicted wholesale power market prices

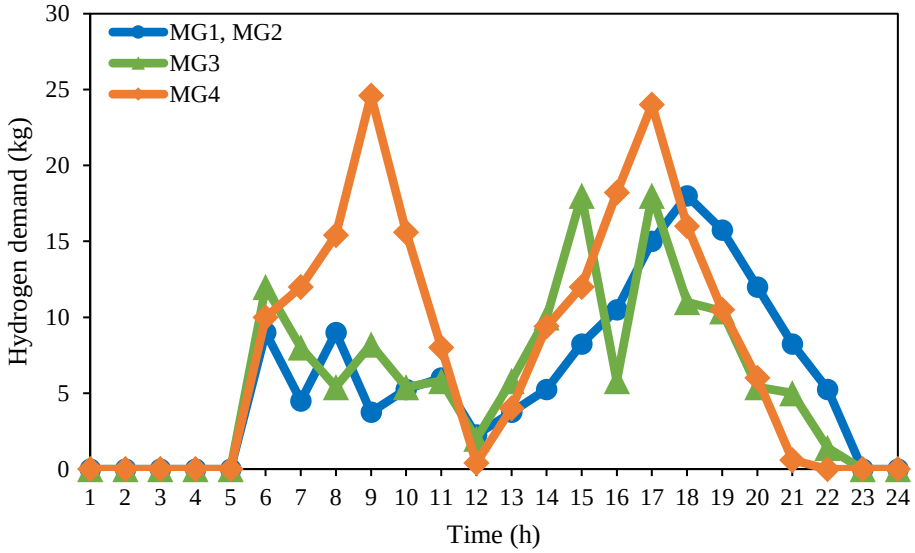

Fig. 5. Hourly predicted hydrogen demand [27]

Table 2. Technical characteristics of energy storage systems

		MG1	MG2	MG3	MG4
ESS	SoC max/min (MW)	2/0.1	2/0.1	2.5/0.1	2.5/0.1
	charge/discharge max (MW)	0.5/0	0.5/0	0.5/0	0.5/0
	charge/discharge min (MW)	0.5/0	0.5/0	0.5/0	0.5/0
	charge/discharge efficiency (%)	95/95	95/95	95/95	95/95
TSS	SoC max/min (MWt)	1.2/0	1.2/0	2/0	2/0
	charge/discharge max (MWt)	0.4/0	0.4/0	0.4/0	0.4/0
	charge/discharge min (MWt)	0.4/0	0.4/0	0.4/0	0.4/0
	charge/discharge efficiency (%)	90/90	90/90	90/90	90/90
HSS	SoC max/min (kg)	60/0	60/0	60/0	60/0
	charge/discharge max (kg)	12/0	12/0	12/0	12/0
	charge/discharge min (kg)	12/0	12/0	12/0	12/0
	charge/discharge efficiency (%)	100/100	100/100	100/100	100/100

Case 1: In this case, the optimization problem was solved in a deterministic manner, and the uncertainty of the wholesale power market was ignored. Fig. 6 depicts transacted power between MGs and coordinating center, where values are negative mean MG imports power and values are positive mean MG exports power. As shown in this figure, buying power from the wholesale power market for the MMG community is negatively correlated with power market prices. All MGs are willing to import power during low price periods (t=1-11, 19, 24) and export power during peak price hours (t=12-18, 20). At hours t=21-23, MGs 2 and 3 export power. However, during the peak price periods, MGs 1 and 4 import power due to high demand.

Fig. 7 indicates the optimal dispatch of power components for each MGs separately. MGs 1 and 4 are equipped with CHP type 2 and MGs 2 and 3 are equipped with CHP type 1. As shown below, MGs with the same type of CHP units run these components almost simultaneously. CHP units of all MGs are called on after hour t=12 due to the rise in the power market prices and the operators prefer to use domestic technologies to supply loads. For MGs 1 and 4, CHP units are online during hours t=5 to t=6. This is due to the fact that the operation cost of power generation for CHP type 2 is lower than power market prices. The operator of each MG benefits from an electrical storage system due to the ability to save power during low price hours and be able to deliver it at peak price hours. According to Fig. 7, ESSs charge during t=1-4, 8-10, 23-24, where the power market prices are low and discharge when prices rise, i.e., t=5-6, 17-21. Power-to-Hydrogen technology is mainly depending on hydrogen demand and the power market for each MG. During initial hours, although there is no hydrogen demand, the conversion of power to hydrogen can be seen. This is due to the fact that power market prices are low during this period and the output hydrogen stores at the hydrogen tank in order to use when necessary. Hydrogen-to-Power conversion for all MGs was conducted only at t=17, and that is also when the power market price is at its highest. Finally, the EV fleets charging and discharging schedule is depicted in Fig. 7. EV fleets as mobile storage systems and have a similar performance of ESS between the time period of the arrival

time and the departure time. During off-peak market price periods which are *t*=1-3, 7-9, 23-24, EV fleets are G2V mode and during on-peak periods (*t*=5-6, 17-21). EV fleets operate in V2G mode.

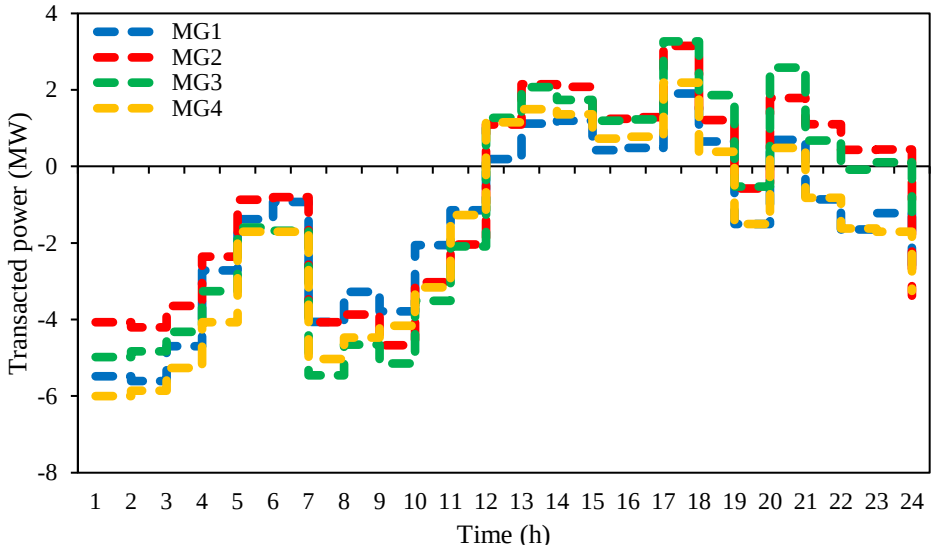

Fig. 6. MGs transacted power with the coordinating center

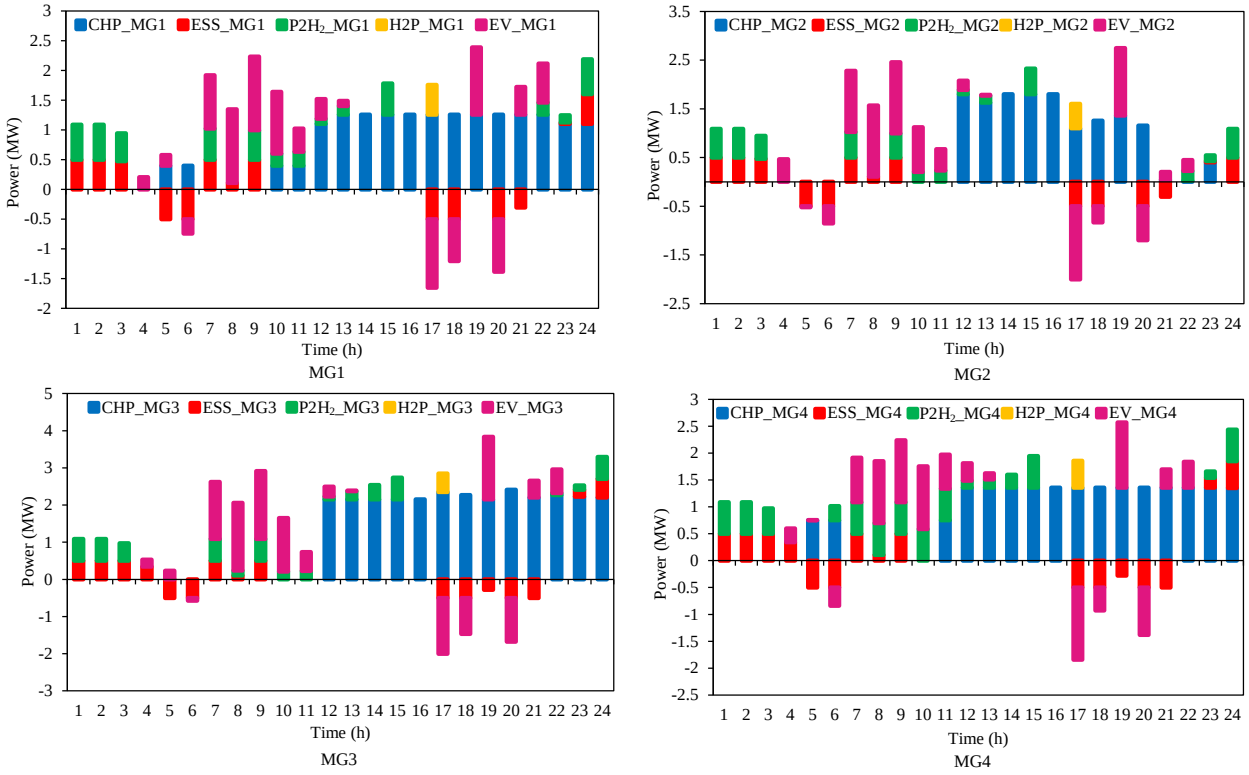

Fig. 7: Hourly optimal dispatch of power for MMG community

Besides the power and hydrogen demand, heat demand needs to be supplied. Fig. 8 illustrates the optimal heat dispatch of components in the MGs. According to the obtained results, at initial hours, Power-to-Heat technology was running due to lower power market prices. The generated heat can be stored in the thermal storage tank. $P2H_2$ was running in all MGs except in MG1 during the initial hours due to high heat demand during this period. After that, the operators of MGs can use boiler or CHP units to supply the heat. The operator of MGs 1 and 2 prefer to run the boiler more than the operators MGs 3 and 4 do. That is due to the fact that generation costs for boilers of MGs 1 and 2 are cheaper. Instead, MGs 3 and 4 benefit from their CHP units at a higher capacity than MGs 1 and 2. Evidently, MGs 1 and 2 use boilers, and if there is only a lack of heat, the CHP units will be on. In contrast, MGs 3 and 4 prioritize the CHP units when it comes to heat generation, and if the heat production from CHP does not satisfy the demands, only then the boilers are switched on. Furthermore, TSS utilities are the other alternatives that assist MGs to supply heat demand. TSSs charging and discharging mainly depend on heat demand and power market due to existing power-to-heat components, e.g., during initial hours, TSSs charges from power-to-heat components and during hours t=5-6 discharge of most TSSs can be seen due to higher prices.

Fig. 9 demonstrates hydrogen storages' state of charge (SOC) and the amount of purchased hydrogen from the HPC. The hydrogen storage systems can only charge from $P2H_2$ technology or by purchasing from the HPC. As demonstrated in the figure, hydrogen storages charge from $P2H_2$ technology at initial hours due to low power market prices. Then during on-peak power market hours and on-peak hydrogen demand hours, HSSs deliver hydrogen. For example, during hours t=16-21, $P2H_2$ technology stopped due to on-peak power market price hours and instead, hydrogen storages discharged. Furthermore, during this period, the lack of hydrogen is compensated by the HPC.

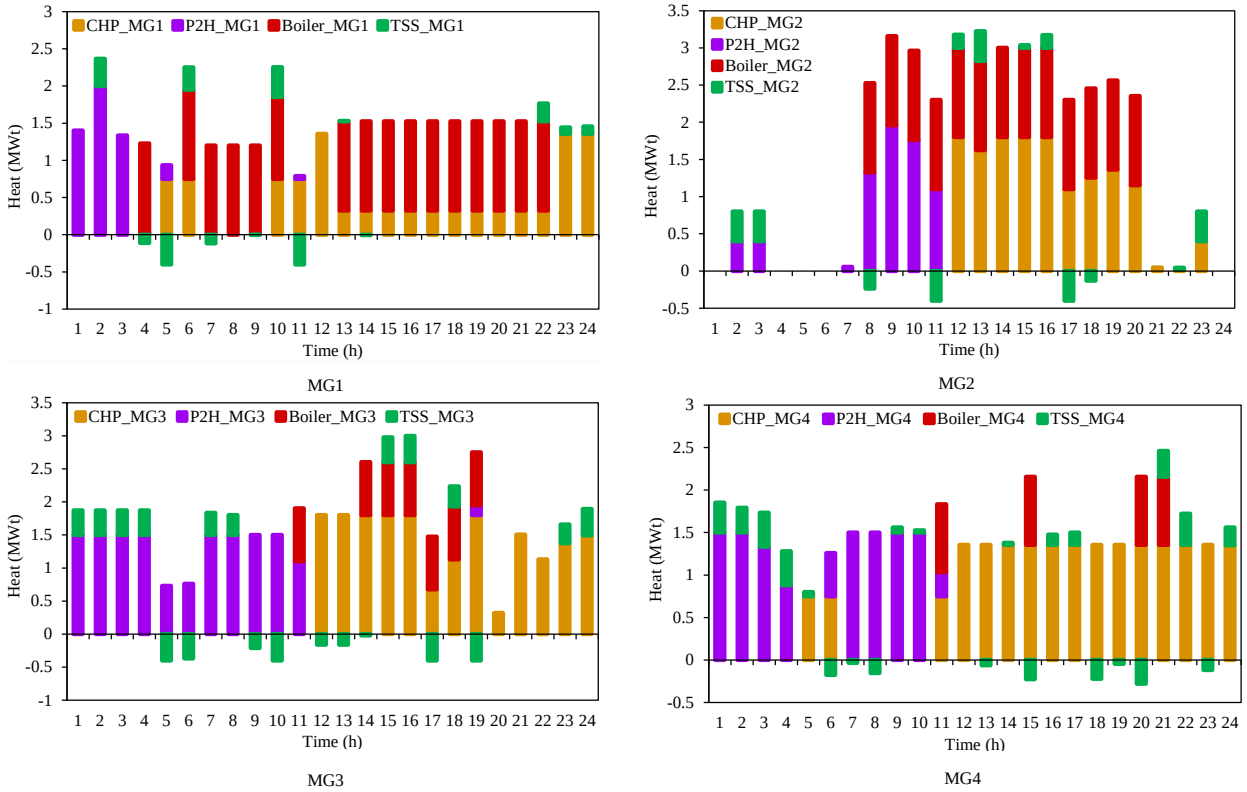

Fig. 8. Hourly optimal dispatch of heat for MMG community

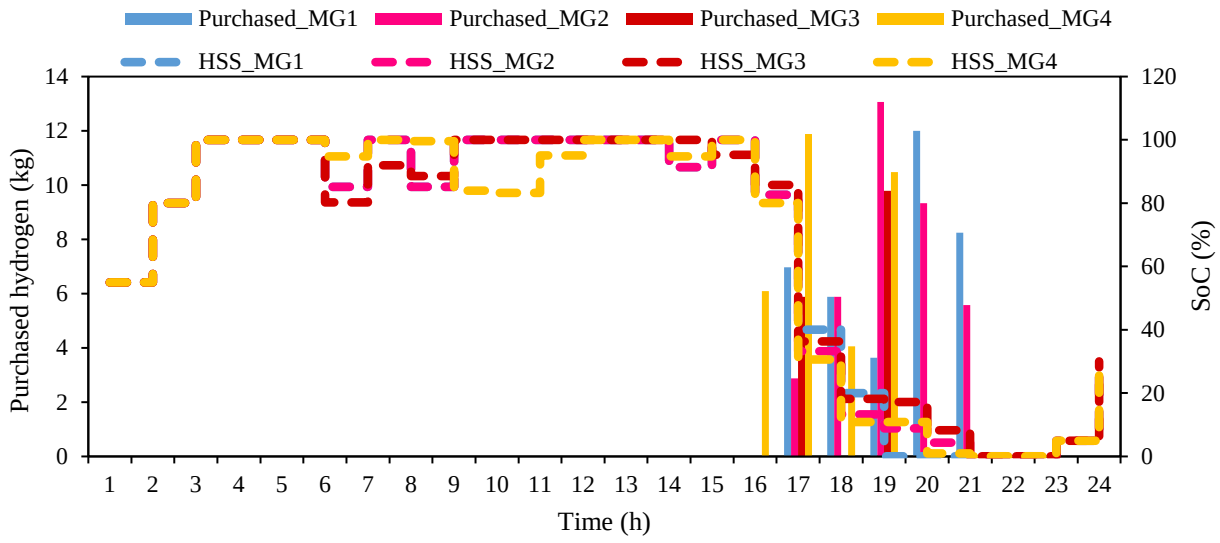

Fig. 9. The optimal hourly state of hydrogen storage systems and the amount of purchased hydrogen

Figs. 10 and 11 show the result of demand response implementation for electrical and thermal demand, respectively. The operators encourage the demand side sector to have a role in the demand response program by sending dynamic power market prices and promoting RES utilization and energy system

stability. According to Fig. 10, electrical demand response was successfully supplied, and the performance during this time period was positive. All the MGs shift their loads from on-peak power market hours, i.e., *t*=13-23, to off-peak hours, i.e., *t*=1-12, 24. In doing so, MGs can benefit by supplying 10% of the loads for a lower cost. In addition, according to the thermal demand response implementation results in Fig. 11, power market prices also affect thermal demand response due to the power-to-heat technology. However, for MG1during hours *t*=13-21, thermal demand was shifted up. This is occurred owing to boiler generation during these hours, which is beneficial to shift up the thermal load.

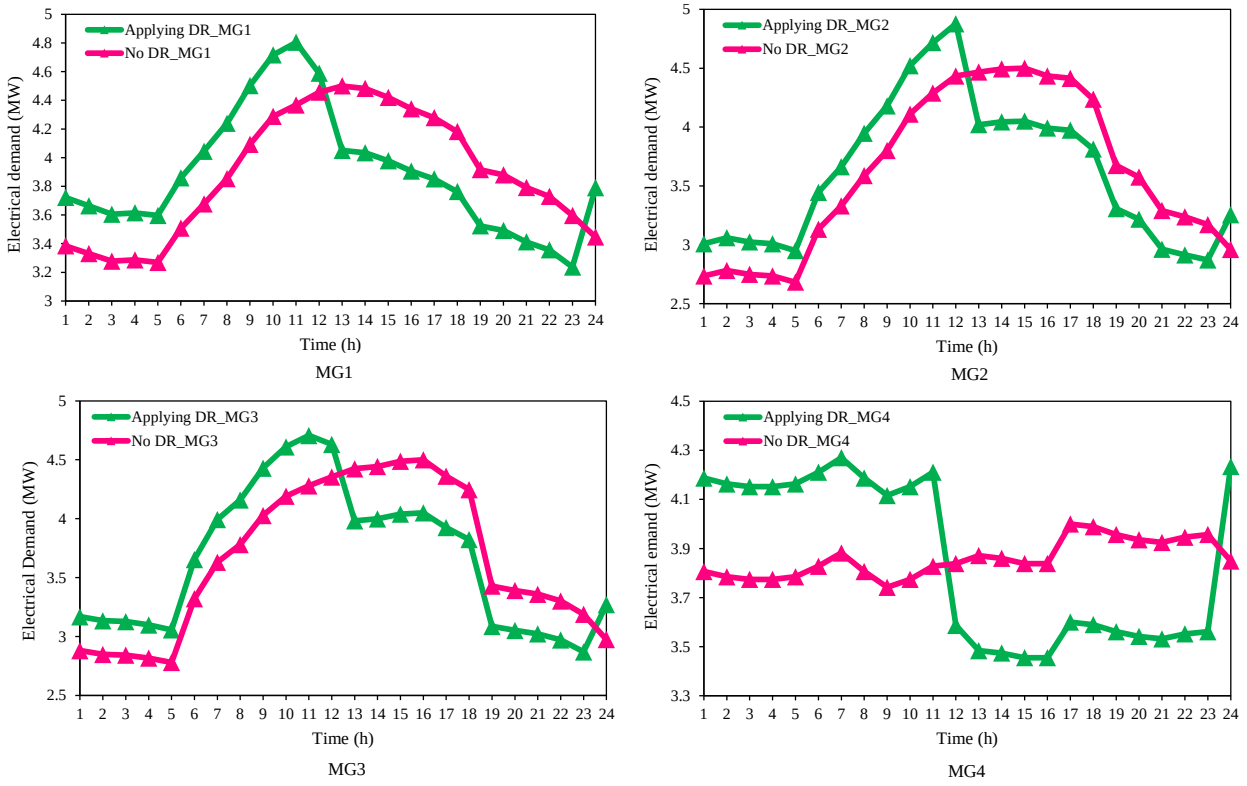

Fig. 10: Electrical demand response performance

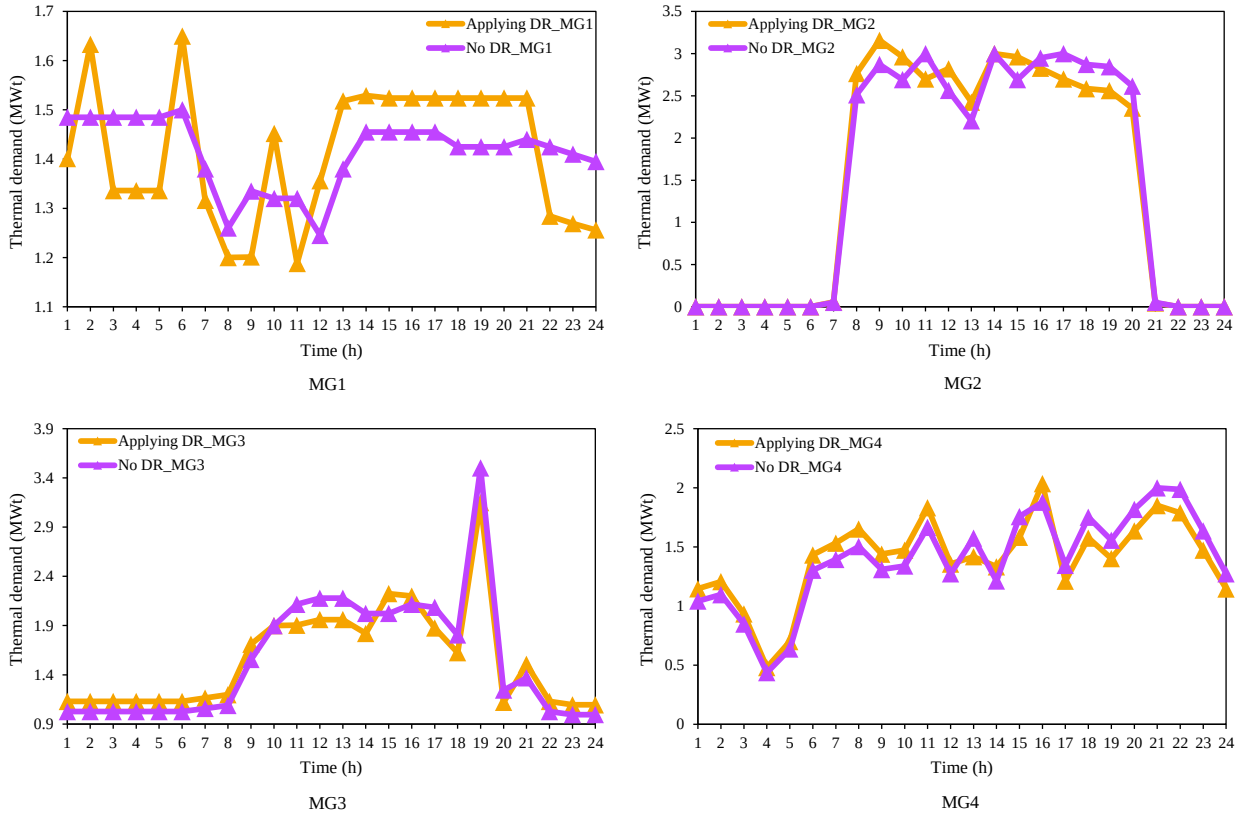

Fig. 11. Thermal demand response performance

In the last part of this case, operation costs of MGs and the contribution of the utilized new emerging flexible sources are analyzed. Table 3 reports operation costs for each MGs and combined cost for the MMG community separately. According to the table, the operation cost of the CHP units has the most shares in the total operation cost, and that is 92%. Also, the share of purchased hydrogen, the operation cost of the boilers, and the cost of the interaction with the power market are 7.42 %, 7 %, and 6.87 %, respectively. Furthermore, the contribution of new emerging flexible sources is depicted in Fig. 12. According to this figure, for MGs 1 and 2, electrical DR has the most impact on the operation cost by 15.36 % for MG1 and 17.88 % for MG2. However, for MGs 3 and 4, ESS shows better performance and has a considerable impact of 43.68 % for MG3 and 36.96 % for MG4. Also, in order to show the performance of the ADMM decomposition, Table 4 and Figure 12 are provided. Table 4 compares obtained results between centralized and decentralized approaches. With a general look at this table, it can be seen that the accuracy of the ADMM technique is quite felicitous and minor deviations from

centralized results are ignorable. Further, Figure 12 presents the ADMM method convergence for each MG individually. As it has been shown, the ADMM could converge very fast for all MGs and this shows its applicability and scalability.

Table 3: Operation costs of each MG

	MG1	MG2	MG3	MG4	MMG community
Purchased power ($)	1109.81	794.28	814.28	1290.90	4009.27
Sold power ($)	643.70	1463.86	1508.24	765.19	4380.99
Purchased hydrogen ($)	121.20	121.20	51.70	107.30	401.40
CHP ($)	821.42	1584.41	1705.88	881.38	4993.09
Boiler ($)	126.60	109.75	88.87	55.54	380.76
Total ($)	1535.33	1145.78	1152.49	1569.93	5403.53

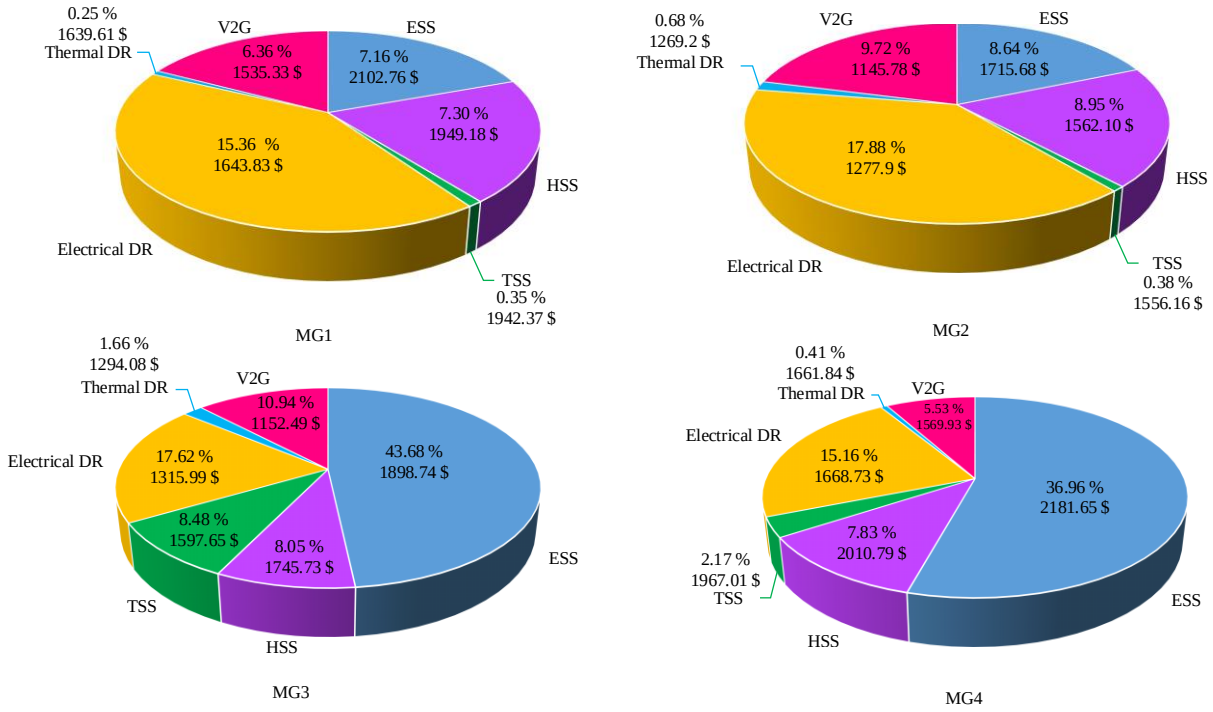

Fig. 12. Contribution of the flexible sources in the MGs' operation cost

Table 4: Comparison of the centralized and decentralized modes

	Decentralized (ADMM)	Centralized
MG1	1535.33	1535.23
MG2	1145.78	1145.66
MG3	1152.49	1152.21
MG4	1569.93	1569.93
MMG Community	5403.53	5403.03

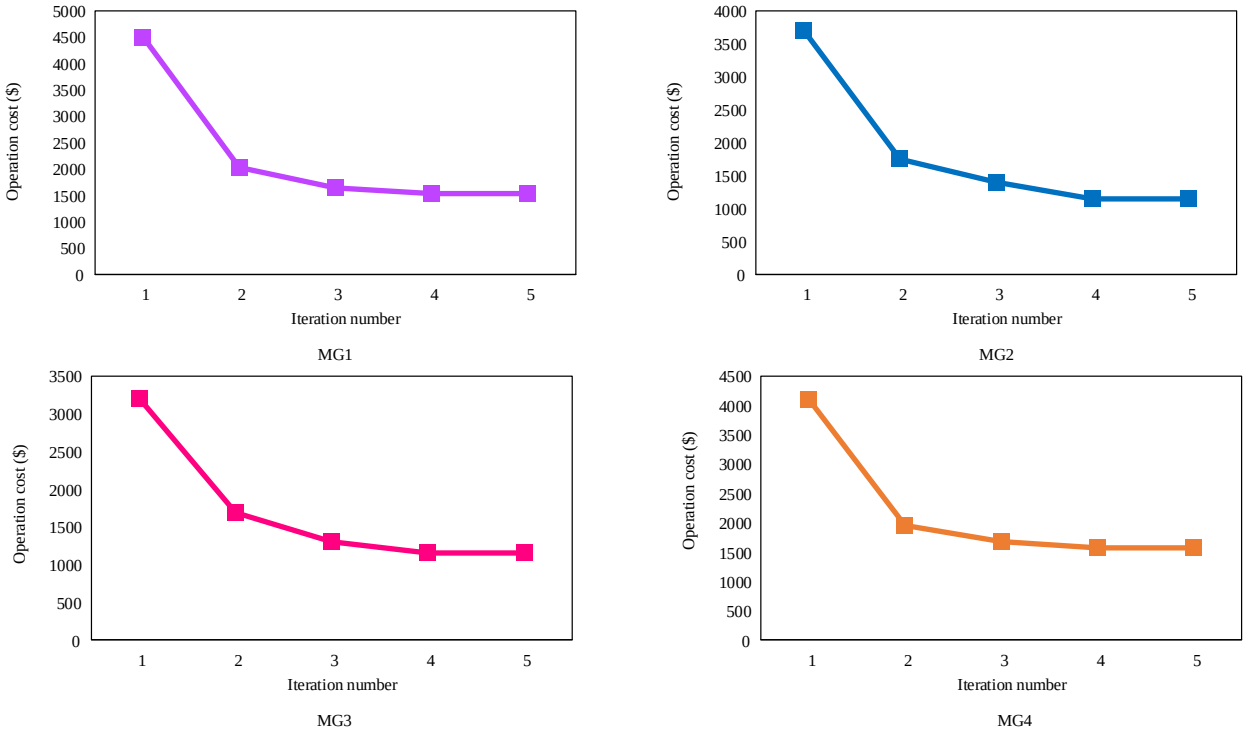

Figure 13. Performance analysis of the ADMM technique for MGs individually

Case 2: The main goal, in this case, is to analyze the wholesale power market uncertainty on the MMG day-ahead scheduling. Thus far, the decentralized robust optimization problem has been solved, and the obtained optimal results are reported below. First of all, wholesale power market uncertainty affects the MMG community transacted power, as depicted in Fig. 14 for different uncertainty budgets. During the worst-case scenarios, the operators behave in a conservative manner, i.e., reduce their interactions with the power market; for example, during hours t=5-6 reduce the imported power, and during hour t=12 reduce the amount of exported power. Figs. 15 and 16 show the uncertainty impact on the hydrogen storage systems and EVs charging and discharging schedules, respectively. The effect of the wholesale power market fluctuations on the MGs' operation costs has been analyzed as presented in Table 5. As the operators have a pessimistic look to the day-ahead predicted prices, operation costs increase to handle the uncertainty in a conservative manner in case of robust optimization. In addition, the more uncertainty budget increases, the more worst-case hours taken into account of the scheduling, so the more operation costs obtain. To further investigate the robust scheduling and its impact on the operation costs, a

sensitivity analysis of the amount of uncertainty budget and price deviation against operation costs was performed, and results are demonstrated in Fig. 17. According to this analysis, price deviation also has a positive correlation in the robust scheduling with incrementation of operation costs. Undeniably any incrementation in the robustness level and price deviation case more robustness manner and results in higher operating costs. In order to verify the optimality of the robust approach, table 6, which contributes to the after-the-fact analysis, has been provided. It has been considered that after the fact, the power market witnesses uncertainty for 5, 10 and 15 worst-case hours, i.e., $\Gamma = 5,10,15$. In a such condition, according to the supplied table, without the robust optimization method imposed operation costs for the MMG community are \$5671.32, \$5801.05, \$5966.73, respectively. However, these values could be reduced via applying the robust method as compared in the table; therefore, the robust optimization is a powerful and effective method for handling the power market uncertainty. In the final section of the results, the performance of the ADMM technique is analyzed. Fig. 18 illustrates the MMG community total operation cost at each iteration for $\Gamma = 5$. As mentioned below, the ADMM technique converges after four iterations, which shows its ability in computational speed and scalability. Furthermore, in Table 7, the ADMM performance is compared with the centralized problem, which confirms the accuracy ADMM technique.

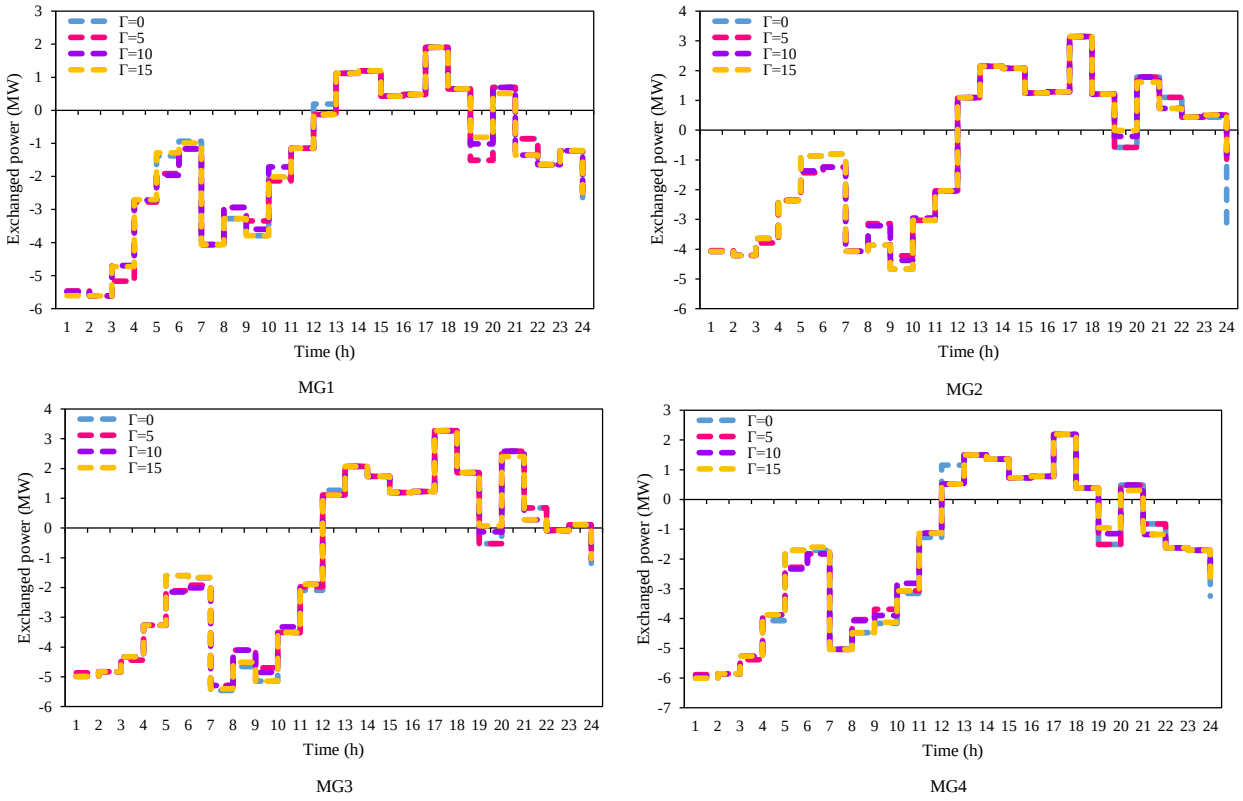

Fig. 14. MMG community transacted power under the uncertainty

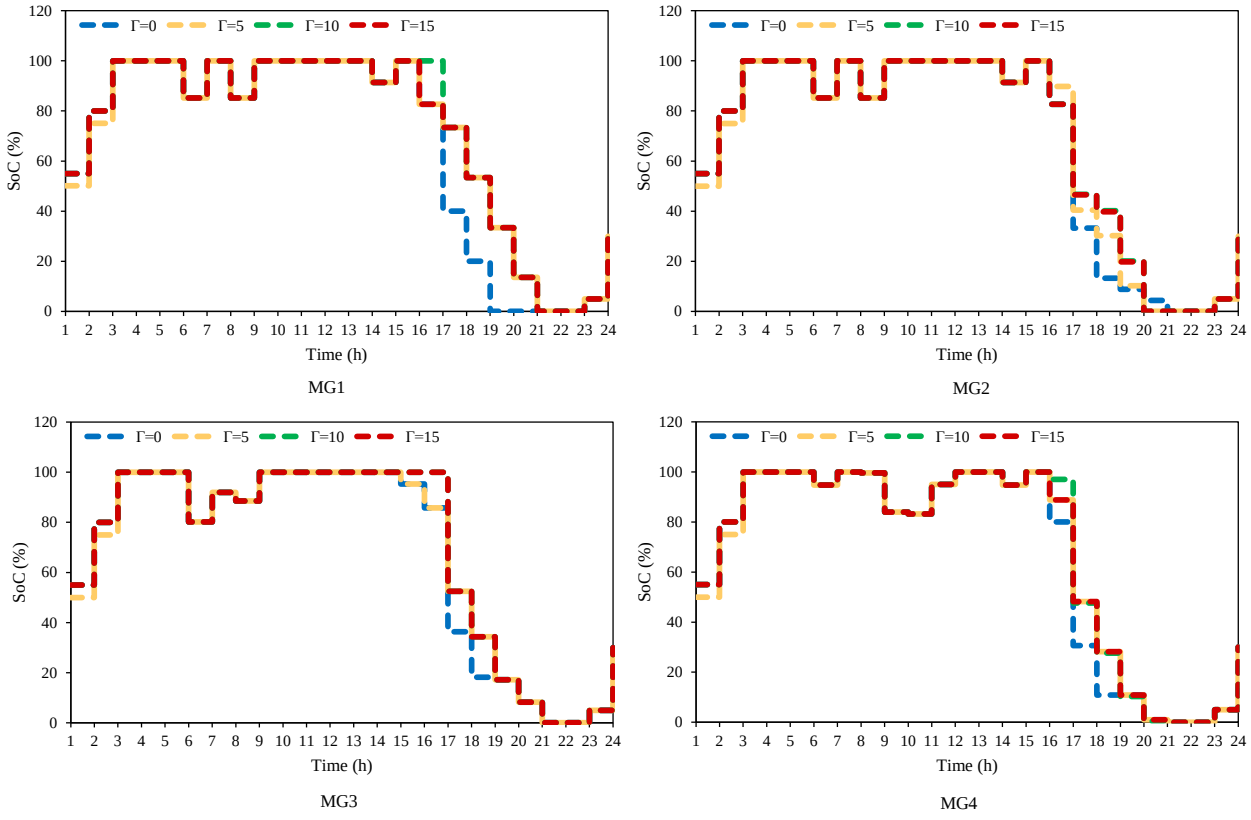

Fig. 15. Hydrogen storage systems SoCs under the uncertainty

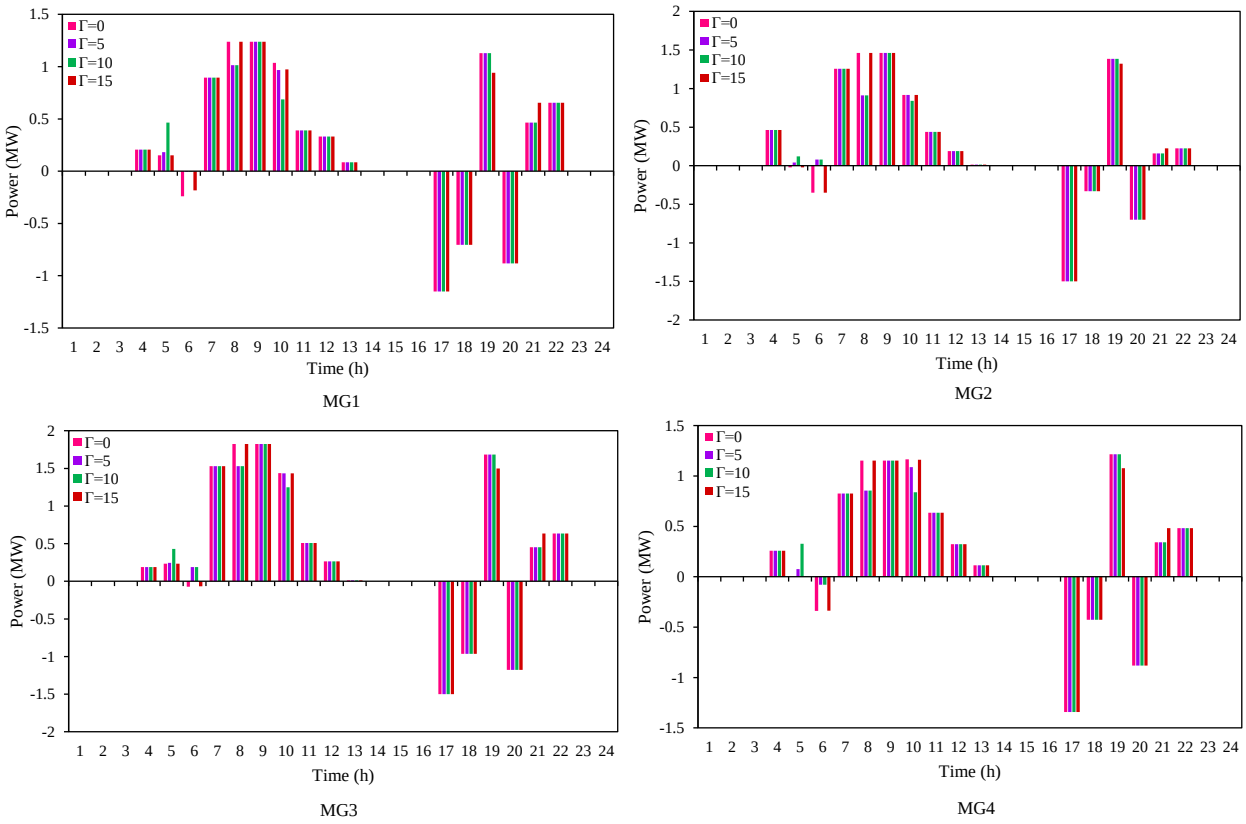

Fig. 16. EVs charging and discharging schedule under the uncertainty

Table 5: Impact of the uncertainty on the operation costs

	MG1 ($)	MG2 ($)	MG3 ($)	MG4 ($)	MMG community ($)
$\Gamma = 0$	1535.33	1145.78	1152.49	1569.93	5403.53
$\Gamma = 5$	1586.65	1188.58	1181.02	1606.61	5562.85
$\Gamma = 10$	1613.39	1211.07	1206.92	1638.74	5670.12
$\Gamma = 15$	1640.25	1226.11	1220.82	1670.22	5757.4

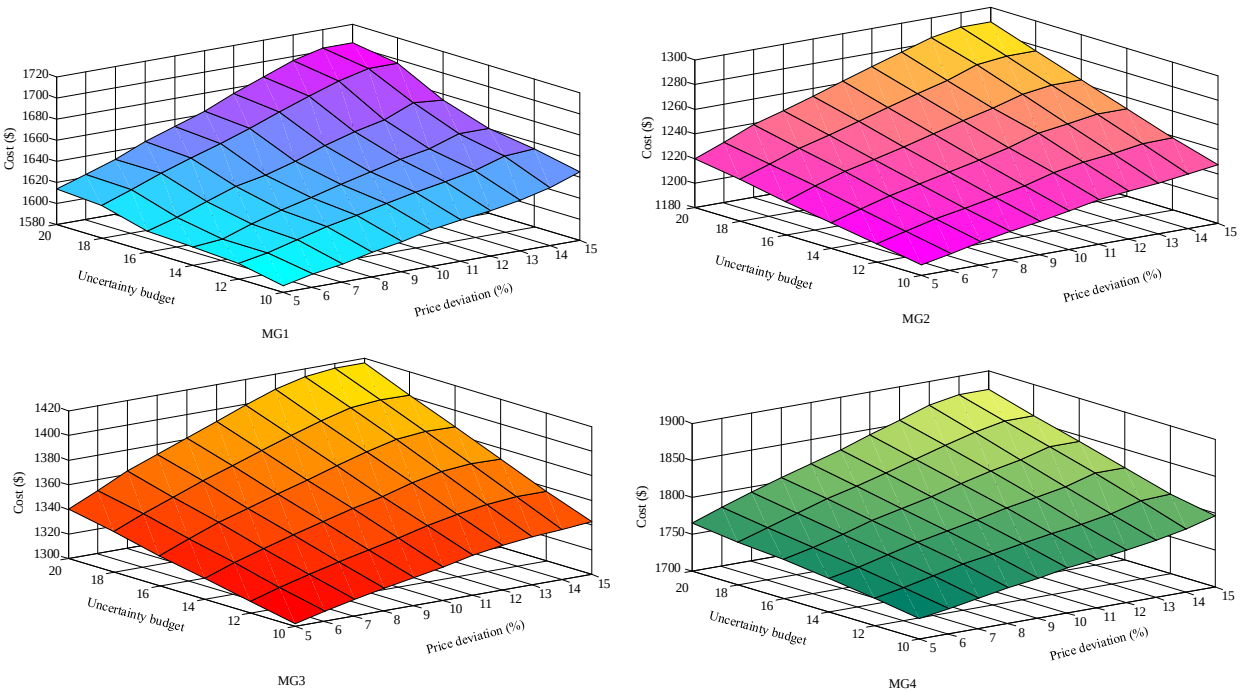

Fig. 17. Sensitivity analysis of robustness level and price deviation against operation cost

Table 6: After the fact analysis without robust optimization and in the case of robust optimization

	No robust optimization ($)	Robust optimization ($)
$\Gamma = 5$	5671.32	5562.85
$\Gamma = 10$	5801.05	5670.12
$\Gamma = 15$	5966.73	5757.4

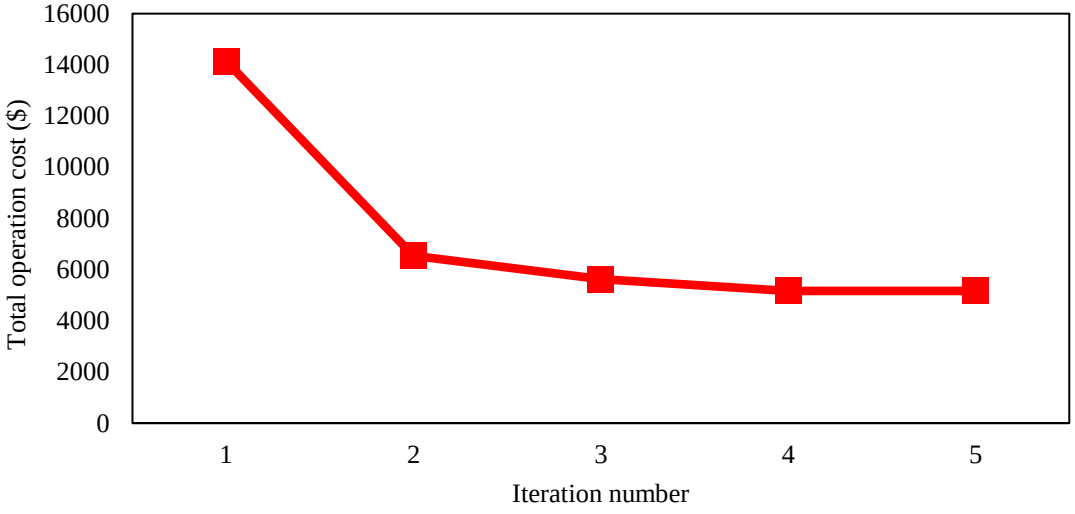

Fig. 18. Performance analysis of the ADMM technique

Table 7: Comparison of the ADMM performance for different uncertainty budgets

MMG community operation cost ($) / Uncertainty budget	Decentralized (ADMM)	Centralized
$\Gamma = 0$	5403.53	5404.03
$\Gamma = 5$	5562.85	5562.91
$\Gamma = 10$	5670.12	5671.47
$\Gamma = 15$	5757.4	5757.13

Conclusion

This paper proposed a robust decentralized energy management platform for optimal day-ahead scheduling of interconnected hydrogen, heat, and power-based microgrids in the presence of hydrogen refueling stations and electric vehicle parking lots. Each microgrid was equipped with a wind turbine, photovoltaic panel, combined heat and power units, boiler, power-to-heat, and power-to-hydrogen technologies, electrical, thermal and hydrogen storage systems. Moreover, microgrids were enabled to participate in demand-side management via electrical and thermal demand response programs. Furthermore, hydrogen refueling stations and electric vehicle parking lots were considered in the microgrids to deliver hydrogen and electric vehicle demands. By using robust optimization to manage the power market uncertainty, operators of microgrids could decide how much risk they would take in the day-ahead scheduling. The alternating direction method of the multipliers (ADMM) approach was introduced to the proposed system to preserve the data privacy and security of the microgrids, to increase the scalability and to handle the optimization problem in a decentralized manner. According to gained results, establishing multi-energy storage systems led to a decrease in the operating costs of microgrids by 34.8%. Applying demand response also showed a positive impact and constituted 7.78 % of microgrids' cost-saving, collectively. In addition, vehicle-to-grid technology of electric vehicles appropriately assisted microgrids and comprised 8.13 % of operation costs of the whole community. Applying robust optimization imposed a risk-averse manner to the microgrids, which each microgrid behaves circumspectly to participate in the power market. Finally, the ADMM, by converging through five

iterations, showed significantly improved performance, which makes the proposed model a promising solution for decentralized systems.

References

[1] https://www.epa.gov/ghgemissions/sources-greenhouse-gas-emissions (accessed.

[2] K. P. Brooks, R. P. Pires, and K. L. Simmons, "Development and validation of a slurry model for chemical hydrogen storage in fuel cell vehicle applications," *Journal of Power Sources*, vol. 271, pp. 504-515, 2014.

[3] Y. Tao, J. Qiu, S. Lai, X. Zhang, and G. Wang, "Collaborative Planning for Electricity Distribution Network and Transportation System Considering Hydrogen Fuel Cell Vehicles," *IEEE Transactions on Transportation Electrification*, 2020.

[4] J. Li, J. Lin, Y. Song, X. Xing, and C. Fu, "Operation optimization of power to hydrogen and heat (P2HH) in ADN coordinated with the district heating network," *IEEE Transactions on Sustainable Energy*, vol. 10, no. 4, pp. 1672-1683, 2018.

[5] A. Mansour-Saatloo, M. A. Mirzaei, B. Mohammadi-Ivatloo, and K. Zare, "A risk-averse hybrid approach for optimal participation of power-to-hydrogen technology-based multi-energy microgrid in multi-energy markets," *Sustainable Cities and Society*, vol. 63, p. 102421, 2020.

[6] M. Nazari-Heris, B. Mohammadi-Ivatloo, G. B. Gharehpetian, and M. Shahidehpour, "Robust short-term scheduling of integrated heat and power microgrids," *IEEE Systems Journal*, vol. 13, no. 3, pp. 3295-3303, 2018.

[7] Z. Li, S. Bahramirad, A. Paaso, M. Yan, and M. Shahidehpour, "Blockchain for decentralized transactive energy management system in networked microgrids," *The Electricity Journal*, vol. 32, no. 4, pp. 58-72, 2019.

[8] D. Wang, J. Qiu, L. Reedman, K. Meng, and L. L. Lai, "Two-stage energy management for networked microgrids with high renewable penetration," *Applied Energy*, vol. 226, pp. 39-48, 2018.

[9] A. Mansour-Saatloo, M. Agabalaye-Rahvar, M. A. Mirzaei, B. Mohammadi-Ivatloo, M. Abapour, and K. Zare, "Robust scheduling of hydrogen based smart micro energy hub with integrated demand response," *Journal of Cleaner Production*, vol. 267, p. 122041, 2020.

[10] W. Su, J. Wang, K. Zhang, and A. Q. Huang, "Model predictive control-based power dispatch for distribution system considering plug-in electric vehicle uncertainty," *Electric Power Systems Research*, vol. 106, pp. 29-35, 2014.

[11] V. Amir, S. Jadid, and M. Ehsan, "Probabilistic optimal power dispatch in multi-carrier networked microgrids under uncertainties," *Energies*, vol. 10, no. 11, p. 1770, 2017.

[12] S. E. Ahmadi and N. Rezaei, "A new isolated renewable based multi microgrid optimal energy management system considering uncertainty and demand response," *International Journal of Electrical Power & Energy Systems*, vol. 118, p. 105760, 2020.

[13] F. H. Aghdam, N. T. Kalantari, and B. Mohammadi-Ivatloo, "A stochastic optimal scheduling of multi-microgrid systems considering emissions: A chance constrained model," *Journal of Cleaner Production*, vol. 275, p. 122965, 2020.

[14] Y. Zhao, J. Yu, M. Ban, Y. Liu, and Z. Li, "Privacy-preserving economic dispatch for an active distribution network with multiple networked microgrids," *IEEE Access*, vol. 6, pp. 38802-38819, 2018.

[15] S.-H. Park, A. Hussain, and H.-M. Kim, "Impact analysis of survivability-oriented demand response on islanded operation of networked microgrids with high penetration of renewables," *Energies*, vol. 12, no. 3, p. 452, 2019.

[16] H. Gao, J. Liu, L. Wang, and Z. Wei, "Decentralized energy management for networked microgrids in future distribution systems," *IEEE Transactions on Power Systems*, vol. 33, no. 4, pp. 3599-3610, 2017.

[17] H. Karimi and S. Jadid, "Optimal energy management for multi-microgrid considering demand response programs: A stochastic multi-objective framework," *Energy*, vol. 195, p. 116992, 2020.

[18] X. Zhou, Q. Ai, and M. Yousif, "Two kinds of decentralized robust economic dispatch framework combined distribution network and multi-microgrids," *Applied Energy*, vol. 253, p. 113588, 2019.

[19] H. Qiu and F. You, "Decentralized-distributed robust electric power scheduling for multi-microgrid systems," *Applied Energy*, vol. 269, p. 115146, 2020.

[20] W. Huang, W. Zheng, and D. J. Hill, "Distributionally robust optimal power flow in multi-microgrids with decomposition and guaranteed convergence," *IEEE Transactions on Smart Grid*, vol. 12, no. 1, pp. 43-55, 2020.

[21] C. Zhang, Y. Xu, Z. Li, and Z. Y. Dong, "Robustly coordinated operation of a multi-energy microgrid with flexible electric and thermal loads," *IEEE Transactions on Smart Grid*, vol. 10, no. 3, pp. 2765-2775, 2018.

[22] Z. Li and Y. Xu, "Optimal coordinated energy dispatch of a multi-energy microgrid in grid-connected and islanded modes," *Applied Energy*, vol. 210, pp. 974-986, 2018.

[23] J. Chen, B. Qi, Z. Rong, K. Peng, Y. Zhao, and X. Zhang, "Multi-energy coordinated microgrid scheduling with integrated demand response for flexibility improvement," *Energy*, vol. 217, p. 119387, 2021.

[24] Y. Wang, L. Tang, Y. Yang, W. Sun, and H. Zhao, "A stochastic-robust coordinated optimization model for CCHP micro-grid considering multi-energy operation and power trading with electricity markets under uncertainties," *Energy*, vol. 198, p. 117273, 2020.

[25] X. Ding, Q. Guo, T. Qiannan, and K. Jermsittiparsert, "Economic and environmental assessment of multi-energy microgrids under a hybrid optimization technique," *Sustainable Cities and Society*, vol. 65, p. 102630, 2021.

[26] L. Ju *et al.*, "A two-stage optimal coordinated scheduling strategy for micro energy grid integrating intermittent renewable energy sources considering multi-energy flexible conversion," *Energy*, vol. 196, p. 117078, 2020.

[27] X. Wu, S. Qi, Z. Wang, C. Duan, X. Wang, and F. Li, "Optimal scheduling for microgrids with hydrogen fueling stations considering uncertainty using data-driven approach," *Applied Energy*, vol. 253, p. 113568, 2019.

[28] X. Xu *et al.*, "Optimal operational strategy for an offgrid hybrid hydrogen/electricity refueling station powered by solar photovoltaics," *Journal of Power Sources*, vol. 451, p. 227810, 2020.

[29] H. Khani, N. A. El-Taweel, and H. E. Z. Farag, "Supervisory Scheduling of Storage-Based Hydrogen Fueling Stations for Transportation Sector and Distributed Operating Reserve in Electricity Markets," *IEEE Transactions on Industrial Informatics*, vol. 16, no. 3, pp. 1529-1538, 2019.

[30] N. A. El-Taweel, H. Khani, and H. E. Farag, "Hydrogen storage optimal scheduling for fuel supply and capacity-based demand response program under dynamic hydrogen pricing," *IEEE Transactions on Smart Grid*, vol. 10, no. 4, pp. 4531-4542, 2018.

[31] F. Alavi, E. P. Lee, N. van de Wouw, B. De Schutter, and Z. Lukszo, "Fuel cell cars in a microgrid for synergies between hydrogen and electricity networks," *Applied Energy*, vol. 192, pp. 296-304, 2017.
[32] C. B. Robledo, V. Oldenbroek, F. Abbruzzese, and A. J. van Wijk, "Integrating a hydrogen fuel cell electric vehicle with vehicle-to-grid technology, photovoltaic power and a residential building," *Applied energy*, vol. 215, pp. 615-629, 2018.
[33] P. Kou, D. Liang, L. Gao, and F. Gao, "Stochastic coordination of plug-in electric vehicles and wind turbines in microgrid: A model predictive control approach," *IEEE Transactions on Smart Grid*, vol. 7, no. 3, pp. 1537-1551, 2015.
[34] Y. Li and K. Li, "Incorporating demand response of electric vehicles in scheduling of isolated microgrids with renewables using a bi-level programming approach," *IEEE Access*, vol. 7, pp. 116256-116266, 2019.
[35] M. E. Demir and I. Dincer, "Cost assessment and evaluation of various hydrogen delivery scenarios," *International Journal of Hydrogen Energy*, vol. 43, no. 22, pp. 10420-10430, 2018.
[36] M. Shahidehpour, X. Wang, C. Shao, X. Wang, Q. Zhou, and C. jia Feng, "Optimal Stochastic Operation of Integrated Electric Power and Renewable Energy with Vehicle-Based Hydrogen Energy System," *IEEE Transactions on Power Systems*, 2021.
[37] X. Lu, Z. Liu, L. Ma, L. Wang, K. Zhou, and N. Feng, "A robust optimization approach for optimal load dispatch of community energy hub," *Applied Energy*, vol. 259, p. 114195, 2020.
[38] N. Nikmehr, "Distributed robust operational optimization of networked microgrids embedded interconnected energy hubs," *Energy*, vol. 199, p. 117440, 2020.
[39] M. Z. Oskouei, B. Mohammadi-ivatloo, M. Abapour, M. Shafiee, and A. Anvari-Moghaddam, "Strategic Operation of a Virtual Energy Hub with the Provision of Advanced Ancillary Services in Industrial Parks," *IEEE Transactions on Sustainable Energy*, 2021.
[40] D. Bertsimas and M. Sim, "Robust discrete optimization and network flows," *Mathematical programming*, vol. 98, no. 1, pp. 49-71, 2003.
[41] G. Liu, Y. Xu, and K. Tomsovic, "Bidding strategy for microgrid in day-ahead market based on hybrid stochastic/robust optimization," *IEEE Transactions on Smart Grid*, vol. 7, no. 1, pp. 227-237, 2015.
[42] E. Castillo, A. J. Conejo, P. Pedregal, R. Garcia, and N. Alguacil, *Building and solving mathematical programming models in engineering and science*. John Wiley & Sons, 2011.
[43] P. Siano, G. De Marco, A. Rolán, and V. Loia, "A survey and evaluation of the potentials of distributed ledger technology for peer-to-peer transactive energy exchanges in local energy markets," *IEEE Systems Journal*, vol. 13, no. 3, pp. 3454-3466, 2019.
[44] W. Zheng, Y. Hou, and Z. Li, "A dynamic equivalent model for district heating networks: formulation, existence and application in distributed electricity-heat operation," *IEEE Transactions on Smart Grid*, vol. 12, no. 3, pp. 2685-2695, 2021.
[45] W. Zheng, W. Wu, Z. Li, H. Sun, and Y. Hou, "A Non-Iterative Decoupled Solution for Robust Integrated Electricity-Heat Scheduling Based on Network Reduction," *IEEE Transactions on Sustainable Energy*, vol. 12, no. 2, pp. 1473-1488, 2021.
[46] W. Zheng and D. J. Hill, "Incentive-based coordination mechanism for distributed operation of integrated electricity and heat systems," *Applied Energy*, vol. 285, p. 116373, 2021.
[47] M. Jalali, K. Zare, H. Seyedi, M. Alipour, and F. Wang, "Distributed model for robust real-time operation of distribution systems and microgrids," *Electric Power Systems Research*, vol. 177, p. 105985, 2019.
[48] S. Boyd, N. Parikh, and E. Chu, *Distributed optimization and statistical learning via the alternating direction method of multipliers*. Now Publishers Inc, 2011.
[49] P. Aliasghari, B. Mohammadi-Ivatloo, and M. Abapour, "Risk-based scheduling strategy for electric vehicle aggregator using hybrid Stochastic/IGDT approach," *Journal of Cleaner Production*, vol. 248, p. 119270, 2020.
[50] S. Hadayeghparast, A. S. Farsangi, and H. Shayanfar, "Day-ahead stochastic multi-objective economic/emission operational scheduling of a large scale virtual power plant," *Energy*, vol. 172, pp. 630-646, 2019.
[51] M. A. Mirzaei, M. Nazari-Heris, B. Mohammadi-Ivatloo, K. Zare, M. Marzband, and S. A. Pourmousavi, "Robust Flexible Unit Commitment in Network-Constrained Multicarrier Energy Systems," *IEEE Systems Journal*, 2020.
[52] M. Ahrabi, M. Abedi, H. Nafisi, M. A. Mirzaei, B. Mohammadi-Ivatloo, and M. Marzband, "Evaluating the effect of electric vehicle parking lots in transmission-constrained AC unit commitment under a hybrid IGDT-stochastic approach," *International Journal of Electrical Power & Energy Systems*, vol. 125, p. 106546, 2021.
[53] L. Sun, W. Liu, B. Xu, and T. Chai, "The scheduling of steel-making and continuous casting process using branch and cut method via CPLEX optimization," in *5th International Conference on Computer Sciences and Convergence Information Technology*, 2010: IEEE, pp. 716-721.
[54] J. Aghaei *et al.*, "Optimal robust unit commitment of CHP plants in electricity markets using information gap decision theory," *IEEE Transactions on Smart Grid*, vol. 8, no. 5, pp. 2296-2304, 2016.
[55] M. Majidi and K. Zare, "Integration of smart energy hubs in distribution networks under uncertainties and demand response concept," *IEEE Transactions on Power Systems*, vol. 34, no. 1, pp. 566-574, 2018.